VI. FLOW REGIME CHARACTERIZATION

Pressure signals and nuclear density gauge signals were recorded during several experiments in both the 0.05 m ID and 0.21 m ID bubble columns. Statistical analysis of the pressure fluctuations and density gauge fluctuations was used to determine flow regimes and flow regime transitions. Wall pressure measurements were made at heights of 0.08, 0.61, 1.22, 1.83, and 2.44 m above the distributor during experiments conducted in both columns. In the 0.05 m ID bubble column, density gauge measurements were made at a fixed height (1.5 m above the distributor); whereas, in the large diameter column, density gauge measurements were made at heights of 0.9, 1.5, and 1.7 m above the distributor. We developed the necessary software that would allow us to do time series analysis of the signals on the Zenith-248 AT compatible computer in our laboratory. The same computer is also interfaced to the data acquisition system (see Chapters II and III) that was used to record the pressure and density gauge fluctuations.

Theoretical Background

Statistical analysis of pressure fluctuations has been used in the past to determine transitions between flow regimes in both two–phase and three–phase bubble columns and fluidized beds. Various techniques may be used to determine flow regimes and flow regime transitions. The two most commonly used designs involving pressure transducers are: (1) measurement of absolute pressure fluctuations and (2) measurement of differential pressure fluctuations. For analysis of systems which operate in the slug flow regime, differential pressure fluctuations can provide more detailed information, and a more accurate measure of the transition from bubbly to slug flow, slug flow to annular flow, and annular flow to mist flow. Differential pressure measurements have generally been limited to two–phase systems (e.g., Ishigai et al., 1965a,b; Lin and Hanratty, 1987;

Matsui, 1984; Miyazaki, et al. 1973; Akagawa, et al. 1971a, b, c). These measurements may be used to determine instantaneous fluctuations in void fraction. The signals returned from differential transducers have the same characteristics as those obtained from a nuclear density gauge or a probe.

Surface pressure fluctuations may be detected with various types of pressure measurement equipment (e.g., pitot tubes, surface mounted transducers, microphones, transducers connected by an external tube, etc.). One drawback associated with surface mounted and tube mounted transducers is that they respond to fluctuations occurring not only in the boundary layer, but also to fluctuations beyond the boundary layer. The tube mounted transducers also suffer from signal delay governed by the length of the tube and the velocity of sound in the medium (Lee, 1983). With tube mounted transducers, it is usually difficult to obtain data over the entire range of frequencies. In general, data obtained from tube mounted transducers will be limited to low frequency fluctuations in the system. For our purpose, this should be sufficient since we are interested in detecting the onset of slug flow.

As discussed by Glasgow et al. (1984), the passage of a buoyant bubble can produce three distinct response characteristics: (1) sound of approach (observable if rapidly rising bubbles are present), (2) pressure field around the object, and (3) wake or vortex street behind the object. Our pressure transducers will only detect fluctuations caused by changes in the pressure field as a bubble passes the surface of the tube (i.e. low frequency oscillations). Even if our system was sensitive enough to detect fluctuations caused by the wakes of bubbles, it would be very difficult, if not impossible, to distinguish between these fluctuations and those created by the pressure field around the bubble.

Three different statistical techniques are commonly employed to determine flow regimes and flow regime transitions from pressure transducer measurements. The statistical analysis involves the use of the power spectral density function (psd), the mean

square error of the pressure fluctuations (MSE), and the probability density function (pdf). The pdf is used extensively in the analysis of signals obtained from differential transducers, nuclear density gauges, and probes. Flow regimes and flow regime transitions cannot be determined directly from pdf's for data obtained from absolute pressure measurements (e.g. Fan et al., 1981; Matsui, 1984;1986; Akagawa et al., 1971a,b,c).

For data from differential pressure measurements and nuclear density gauge measurements, the pdf has significantly different characteristics for different flow regimes. In bubbly flow the pdf is concentrated near a pressure difference (or count rate) corresponding to low gas hold–up. However, when slugs begin to appear, two peaks (or regions) are observed on the pdf curve, one corresponding to low hold–up and the other corresponding to high hold–up. The low hold–up region corresponds to the liquid slugs and the high hold–up region corresponds to the gas slugs. In annular flow, the low hold–up peak disappears and only the peak corresponding to high gas hold–up is observed (Matsui, 1984).

As mentioned previously, the pdf of an absolute pressure signal cannot be used as a direct measure of flow regime transitions. However, the pdf of an absolute pressure signal will broaden as turbulence increases (Patel, 1985). In other words, the variance of the pressure fluctuations in the column changes with gas and liquid velocities, and this change is reflected by an increase or decrease in the variance of the pdf. Two quantities which have found some use in determining flow regime transitions and changes in turbulence are the mean square error (MSE) and root mean square (RMS) of the pressure fluctuations. The MSE is defined as:

$$MSE = \frac{\left[\sum (P_i - \overline{P})^2 / N\right]^{1/2}}{\overline{P}} \qquad i = 1, \ldots, N \tag{6.1}$$

where N is the total number of data points, P_i is the pressure corresponding to data point i, and $\overline{P}$ is the average pressure defined as:

$$\overline{P} = \frac{\sum P_i}{N} \qquad i = 1, \ldots, N$$

Fan et al. (1984) had reasonable success in using this quantity to determine flow regime transitions in a three-phase fluidized bed. Lee (1983) used the RMS, defined as :

$$RMS = (MSE)(\overline{P}) \tag{6.2}$$

to obtain a qualitative description of turbulence in an air lift bubble column.

Two other statistical quantities which are sometimes used are the autocorrelation function and the power spectral density function (psd). The psd is the Fourier transform of the autocorrelation function. The autocorrelation function is the normalized autocovariance function. The autocovariance function gives an indication of how the dependence between adjacent values in a stochastic process changes with lag (u) and is defined as (Jenkins and Watts, 1968):

$$\gamma_{xx}(u) = E[(x(t) - \mu)(x(t+u) - \mu)] = cov[x(t), x(t+u)] \tag{6.3}$$

where E[y] is the expected value of y, cov is the covariance, μ is the mean of the time series, x is the measured quantity (pressures for our case), and u is the lag between observations. The autocorrelation function is given by:

$$\rho_{xx}(u) = \frac{\gamma_{xx}(u)}{\gamma_{xx}(0)} \tag{6.4}$$

where $\gamma_{xx}(u)$ is the autocovariance function evaluated at lag u and $\gamma_{xx}(0)$ is the autocovariance function evaluated at lag 0, or more simply, the variance of the time series. Thus, the RMS is the square root of the autocovariance function evaluated at lag 0, and the MSE is the square root of the autocovariance function evaluated at lag 0 divided

by the mean of the time series (or, for our case, the mean of the pressure fluctuations or density gauge fluctuations).

Fourier transforms are used to approximate the time series. A series of periodic functions may be used to approximate a non–periodic signal. One such series is the Fourier series, in which the periodic functions are sines and cosines. Thus, the Fourier series may be used to approximate the actual pressure signal. In essence, we are fitting the raw signal to a Fourier series. From this type of a fit, we gain information on the periodicity of the signal. Fourier series have the important property that an approximation consisting of a given number of terms achieves the minimum mean square error between the signal and approximation, and also, since they are orthogonal, the coefficients may be determined independently of one another. The sample spectrum is the Fourier transform of the sample autocovariance function. It shows how the average power or variance of the signal is distributed over frequency. Fourier analysis breaks down when applied to time series because it is based on the assumption of fixed amplitudes, frequencies, and phases. Thus, the sample spectrum of a time series can be quite erratic in nature. However, if we treat the sample spectrum as a random variable, and examine its moments, we will be able to explain the erratic behavior. The power spectrum is defined as the first moment, or mean, of the sample spectrum. The power spectral density function is a normalized version of the power spectrum. The psd is the Fourier transform of the autocorrelation function and is defined by (Jenkins and Watts, 1968):

$$P(f) = \int_{-\infty}^{\infty} \rho_{xx}(u)\exp(-j2\pi fu)du \qquad (6.5)$$

Thus, all three quantities (i.e., RMS or MSE, autocorrelation and psd) are related. For our data, we will only use the MSE and psd to show qualitatively, the transitions between flow regimes for various experimental data.

Taitel et al. (1981) presented various correlations for the prediction of flow regime transitions in two–phase gas–liquid flow. By treating our three–phase system as a two–phase system (i.e., using slurry properties in place of liquid properties), we can use Taitel et al.'s correlations to obtain approximate values for the transitions between bubbly and slug flow in the 0.05 m ID bubble column. According to Taitel et al., for our system and range of operating conditions in the 0.05 m ID bubble column, there are two possible flow regimes which can exist, bubbly and slug flow. Taitel et al. also present a correlation for describing the entrance region in which mixing (i.e. churn flow) will exist due to the incoming gas (i.e., in the lower section of the column there will be churn flow, but towards the top of the column slug flow will exist).

According to Taitel et al., bubbly flow will not exist if the following correlation is satisfied:

$$\left[\frac{\rho_{s\ell}^2 g D_{col}^2}{(\rho_{s\ell}-\rho_g)\sigma}\right]^{1/4} \leq 4.36 \qquad (6.6)$$

where $\rho_{s\ell}$ is the density of the slurry, D_{col} is the column diameter, ρ_g is the density of the gas, and σ is the surface tension of the liquid. Note that in their original correlation they used the density of the liquid and not the density of the slurry. For the small diameter bubble column, the quantity on the left hand side of Eq. 6.6 ranges from approximately 5.2 to 5.5. Thus, for our system, according to Taitel et al., it is possible to observe the bubbly regime.

Assuming that the transition to slug flow occurs when the gas hold–up is approximately 25 %, Taitel et al. propose that the following correlation can be used to determine the transition to slug flow:

$$U_{s\ell} = 3.0U_g - 1.15\left[\frac{g(\rho_{s\ell}-\rho_g)\sigma}{\rho_{s\ell}^2}\right]^{1/4} \qquad (6.7).$$

where $U_{s\ell}$ is the superficial slurry velocity and U_g is the superficial gas velocity at which the transition takes place. For the various systems and operating conditions used in

this study, the transition from the bubbly to slug flow regime should occur between gas velocities of 0.048 and 0.056 m/s.

Taitel et al. also present a correlation for predicting the entry region over which churn flow will exist. In this region, it is assumed that short Taylor bubbles are created. Two of these coalesce to form a "large" Taylor bubble (or slug). The entry region is the region in which this coalescence takes place and is defined by:

$$\frac{l_e}{D_{col}} = 40.6\left[\frac{U_m}{\sqrt{gD_{col}}} + 0.22\right] \tag{6.8}$$

For our system, the entry length, l_e ranges from approximately 0.7 m at a gas velocity of 0.06 m/s to 1.0 m at a gas velocity of 0.12 m/s. Thus, if Taitel et al.'s correlations (i.e., Eqs. 6.7 and 6.8) hold true for our system, we should observe a transition to slug flow between gas velocities of 0.04 and 0.06 m/s for all experiments, and furthermore, we should not observe slugs in the lower (0.7 to 1.0 m) section of the bubble column.

The range of gas velocities at which the transition from bubbly to slug flow occurs based on the correlations presented by Taitel et al., agrees with the range of velocities predicted by Deckwer et al., 1980 (see Figure 2.12). Based on the flow regime map presented by Deckwer et al., the transition from the bubbly to churn–turbulent flow regime in the 0.21 m ID bubble column occurs between gas velocities of 0.04 and 0.07 m/s.

Discussion Of Results

Wall pressure fluctuations and nuclear density gauge fluctuation measurements were made in both the small diameter and large diameter stainless steel bubble columns. Raw output (i.e. voltages) from the density gauges and pressure transducers were recorded on the Zenith AT personal computer. The data were then analyzed to obtain the MSE, pdf, and psd. The spectral density functions, psd, were obtained using the IMSL routine PFFT.

Figures 6.1a and 6.1b show typical raw signals from the nuclear density gauge obtained during experiments in the 0.05 m ID bubble column at gas velocities of 0.02 and 0.06 m/s, respectively. The large peaks in each figure correspond to the passage of large bubbles across the beam path of the density gauge. The regularity of the large peaks is significantly different at the two gas velocities. At 0.02 m/s, the large peaks appear randomly and also are less frequent; however, at a gas velocity of 0.06 m/s, they appear at an increased regularity, and also have a relatively higher intensity (amplitude) than those at 0.02 m/s. This regularity indicates the presence of slugs in the dispersion at a gas velocity of 0.06 m/s. At the lower gas velocity (0.02 m/s), the bubbles are smaller and are randomly dispersed in the flow field. Additionally, the lower amplitude of the oscillations at this gas velocity is indicative of the larger liquid fraction at 0.02 m/s relative to that at 0.06 m/s. Figure 6.2 shows typical density gauge fluctuations during experiments in the 0.21 m ID column. The large peaks in Figures 6.2a and 6.2b correspond to the passage of large bubbles through the beam of radiation at gas velocities of 0.02 and 0.12 m/s, respectively. The fluctuations at a gas velocity of 0.02 m/s in the 0.21 m ID column appear similar to those in the 0.05 m ID column at the same velocity. However, at a gas velocity of 0.12 m/s in the 0.21 m ID column, peaks appear randomly; whereas, in the 0.05 m ID column the peaks occur regularly during slug flow (see Figure 6.1b). This non–regularity in peaks at a relatively high gas velocity indicates the presence of the churn–turbulent flow regime. At a gas velocity of 0.12 m/s, the amplitude of the peaks is higher than at a gas velocity of 0.02 m/s, thus indicating the presence of either larger bubbles or swarms of bubbles at this velocity.

Figures 6.3 and 6.4 show typical probability density functions of the pressure signals in the 0.05 and 0.21 m ID column, respectively. Figures 6.3a and 6.4a correspond to the homogeneous bubbly regime. The homogeneous bubbly regime is characterized by a narrow density distribution function. As the gas flow is increased, the pressure variation

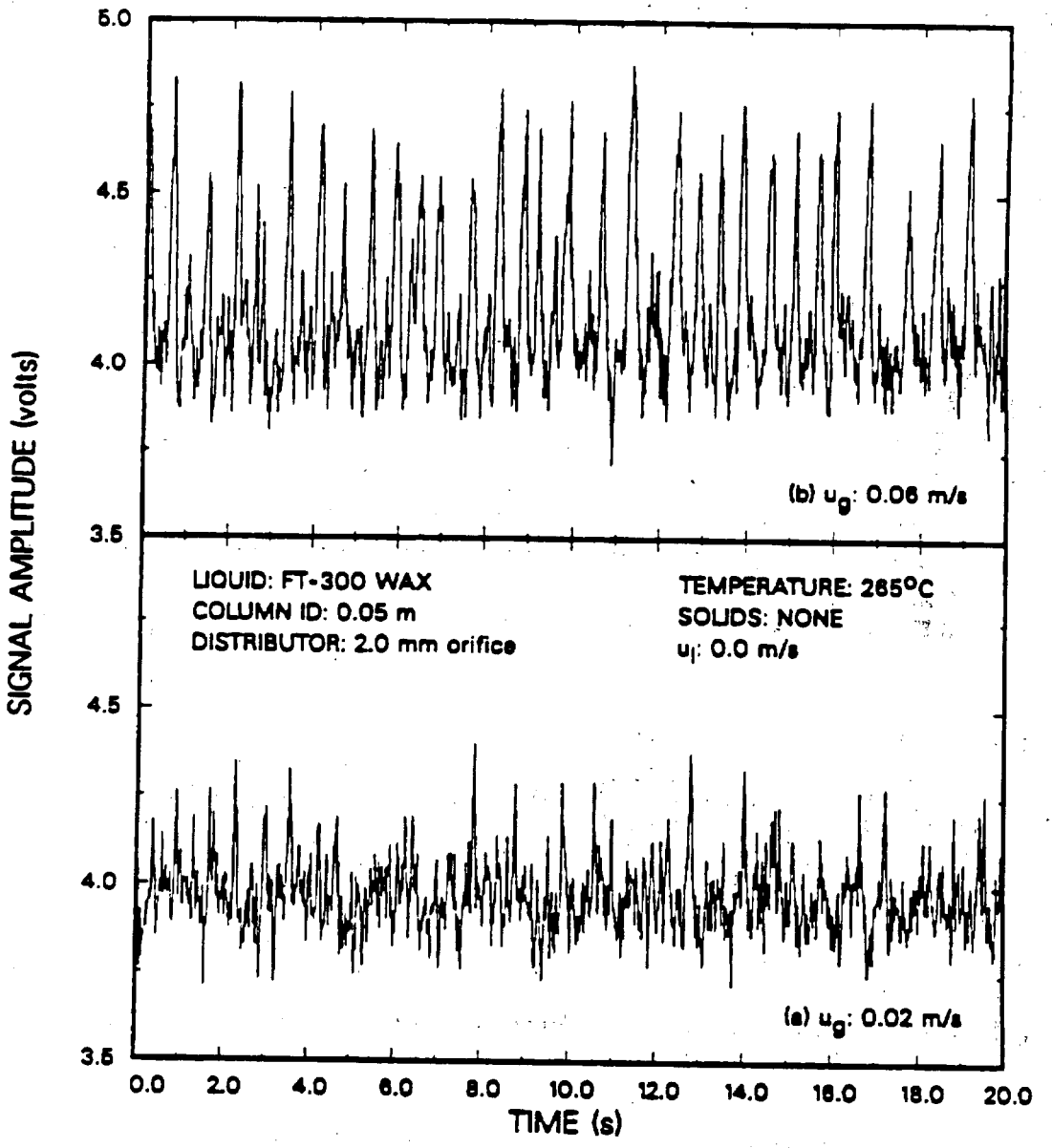

Figure 6.1. Typical raw signals from the nuclear density gauge apparatus during experiments in the 0.05 m ID bubble column.

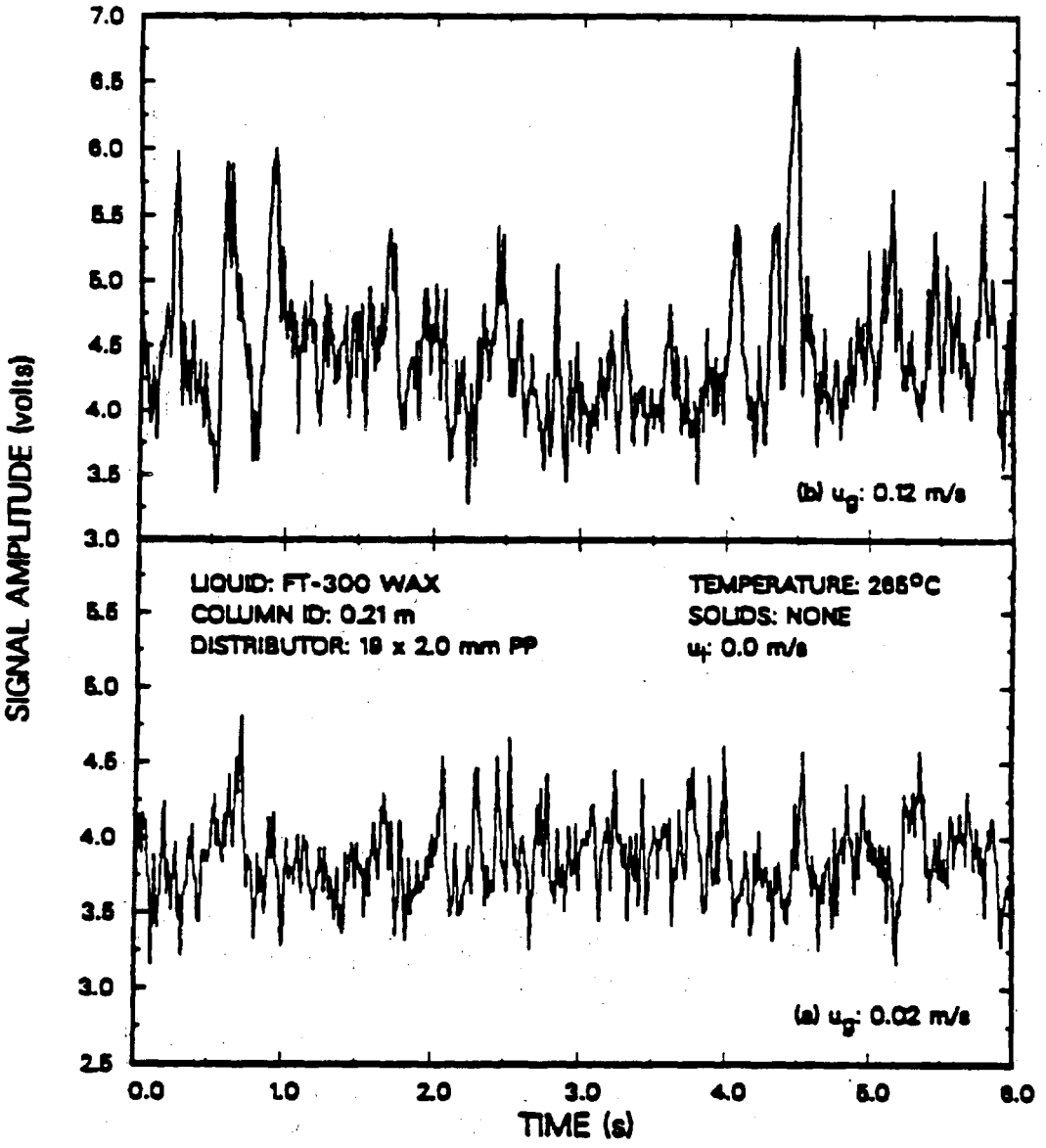

Figure 6.2. Typical raw signals from the nuclear density gauge apparatus during experiments in the 0.21 m ID bubble column.

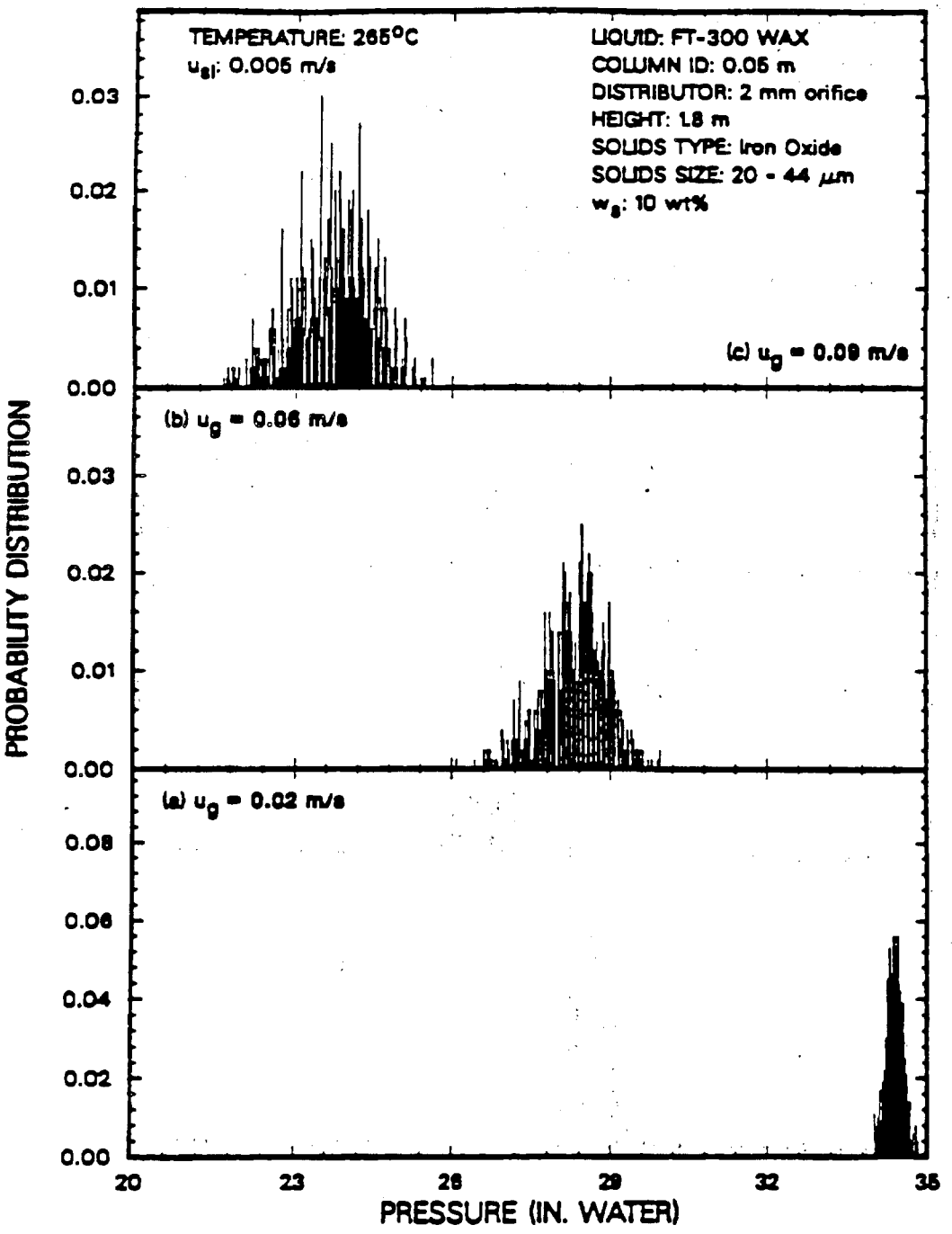

Figure 6.3. Effect of superficial gas velocity on the probability density function from the pressure transducer in the 0.05 m ID bubble column at a height of 1.8 m above the distributor.

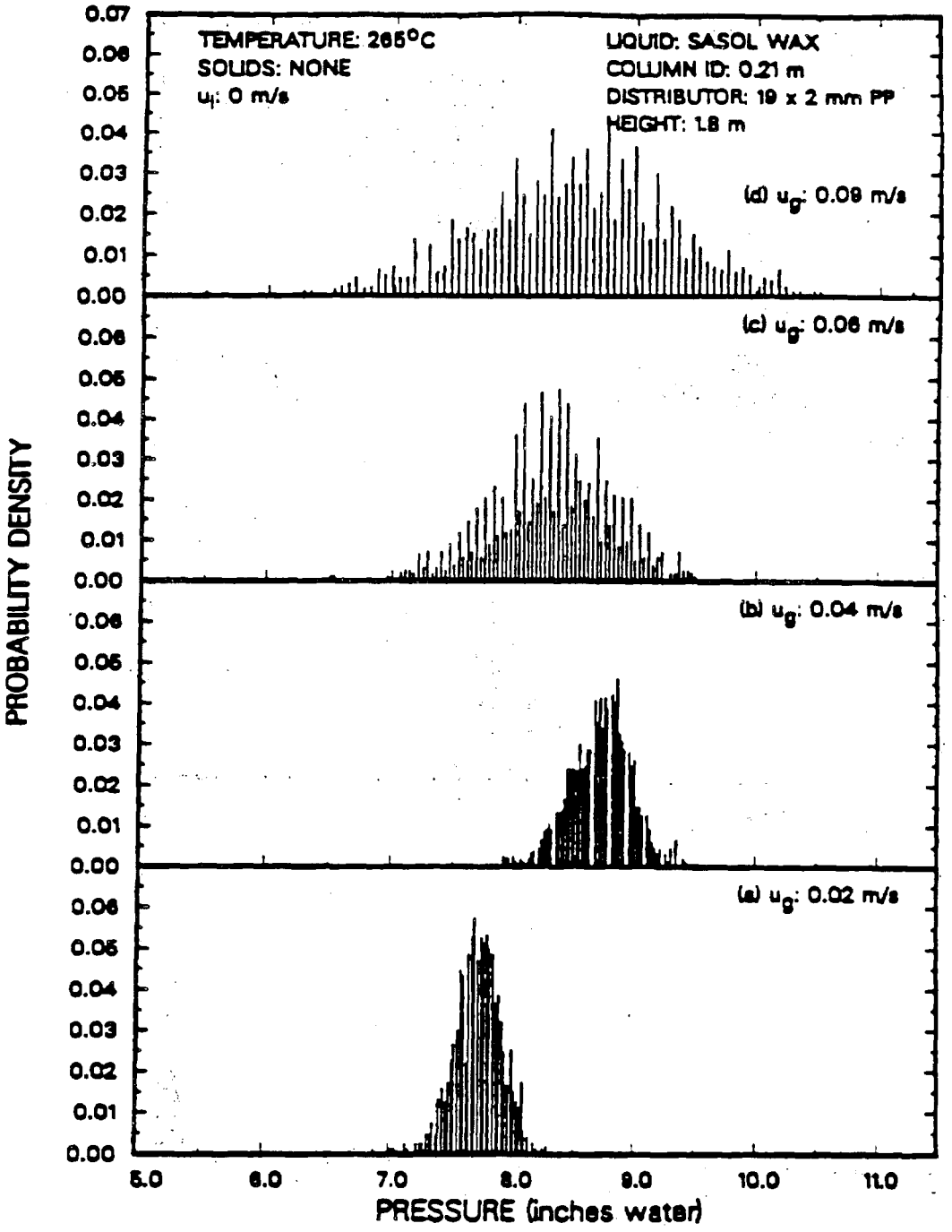

Figure 6.4. Effect of superficial gas velocity on the probability density function from the pressure transducer in the 0.21 m ID bubble column at a height of 1.8 m above the distributor.

increases. As the gas flow is increased to 0.04 m/s, the variation in pressure begins to increase in the 0.21 m ID column (see Figure 6.4b). This slight increase may correspond to the transition regime between bubbly and churn-turbulent flow. At gas velocities of 0.06 and 0.09 m/s in both columns, the variation in pressure increases significantly, indicating the presence of slug flow in the small diameter column and churn-turbulent flow in the large diameter column.

Typical probability density functions from the nuclear density gauges, associated with experiments in the small diameter and large diameter bubble columns, are shown in Figures 6.5 and 6.6, respectively. As mentioned previously, nuclear density gauge fluctuations correspond to fluctuations in gas holdup. The distribution at a gas velocity of 0.02 m/s in both columns has the shape of a normal distribution and can be associated with the homogeneous bubbly regime. As the gas velocity is increased in the small diameter column, the Gaussian distribution becomes skewed to the right (e.g. u_g=0.04 m/s). At a gas velocity of 0.06 m/s, the formation of a second peak is evident at the right hand end of the distribution, and this is exemplified at 0.09 m/s (see Figures 6.5c and 6.5d). An increase in peak intensity corresponds to an increase in the volume fraction of gas. Thus, the second peak at gas velocities of 0.06 and 0.09 m/s corresponds to the presence of slugs. In the large diameter column at gas velocities of 0.08 and 0.12 (see Figures 6.6b and 6.6c, respectively), the distribution becomes skewed to the right also. However, the second peak is not formed. This is expected, since in the churn-turbulent flow regime, the passage of large bubbles is not as regular as it is in the slug flow regime.

Flow Regime Transitions Based on the MSE

MSE were calculated from the raw pressure signal data for all runs conducted in the 0.05 m ID column. In general, the MSE increased with increasing gas velocity and with increasing height above the distributor, but decreased with increasing liquid velocity.

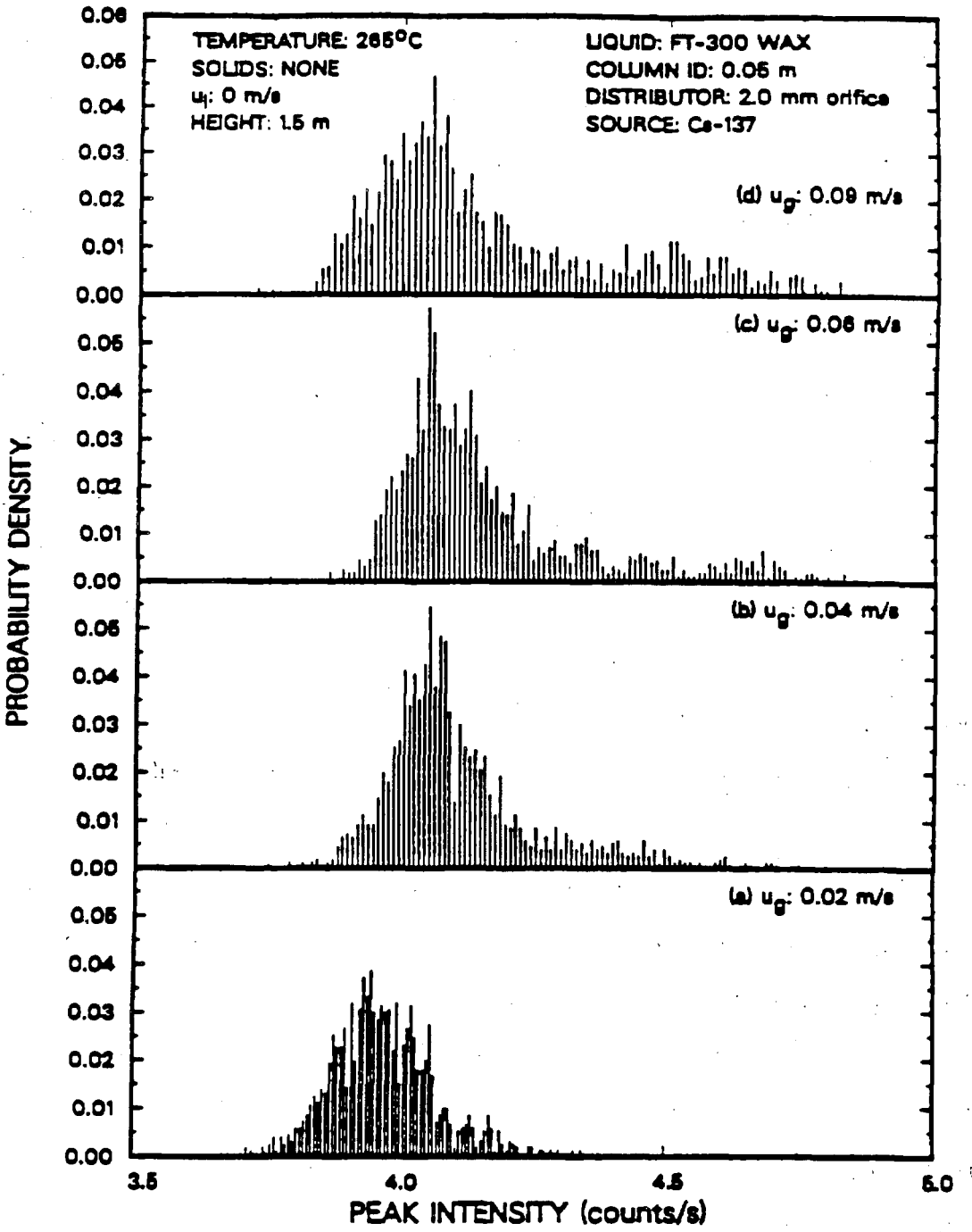

Figure 6.5. Effect of superficial gas velocity on the probability density function from the nuclear density gauge using the Cesium-137 source in the 0.05 m ID bubble column at a height of 1.5 m above the distributor.

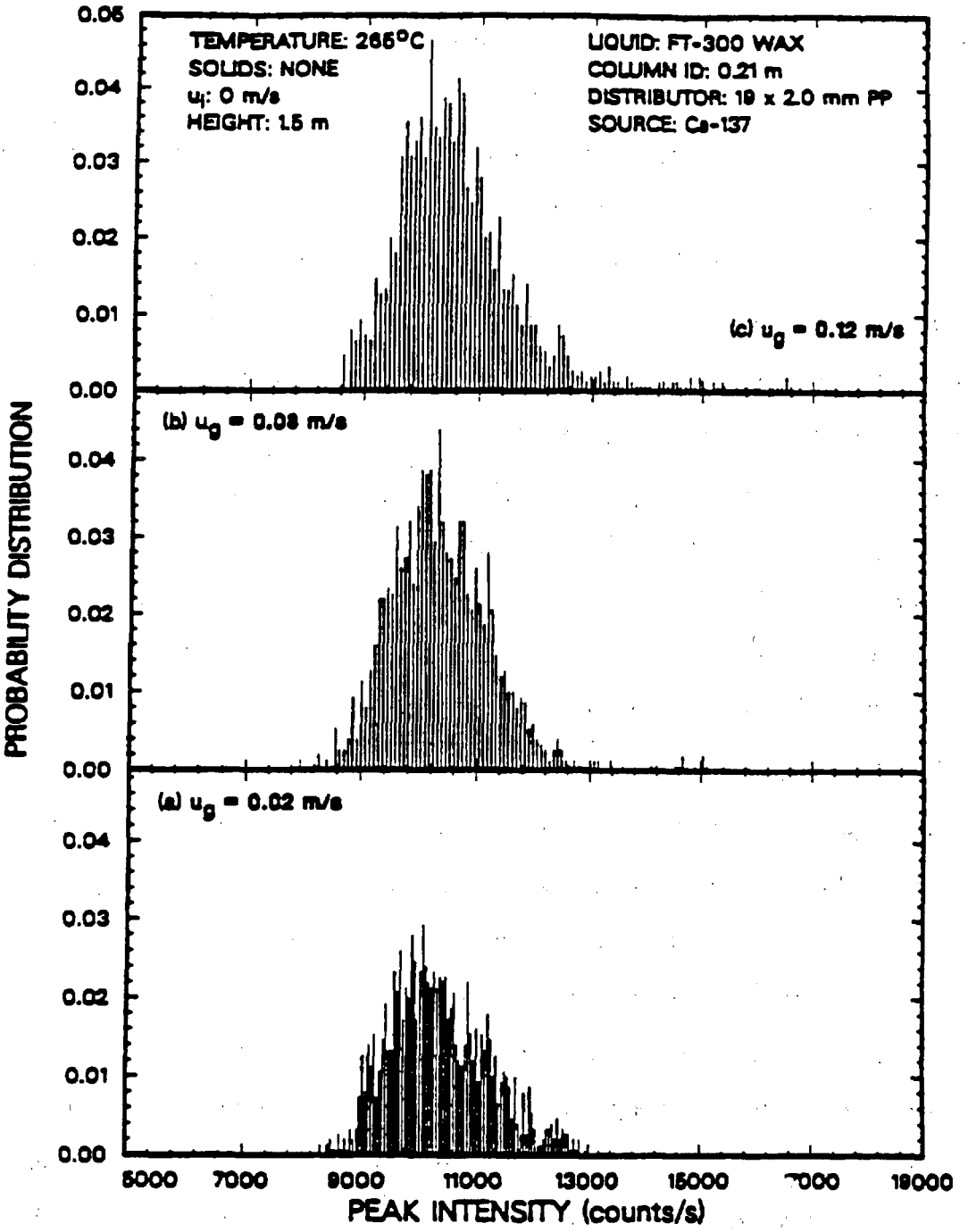

Figure 6.6. Effect of superficial gas velocity on the probability density function from the nuclear density gauge using the Cesium-137 source in the 0.21 m ID bubble column at a height of 1.5 m above the distributor.

Figure 6.7 shows the MSE obtained at a height of 1.2 m for experiments conducted with 0 – 5 μm silica particles at slurry velocities of 0, 0.005, and 0.02 m/s. At low gas velocities (i.e., $u_g \leq 0.06$ m/s, the MSE of the pressure fluctuations is essentially the same for all three experiments. However, at gas velocities of 0.09 and 0.12 m/s the MSE of the pressure fluctuations are significantly different for the various experiments. The MSE for the experiment conducted in the batch mode of operation is significantly higher than those for the other two runs, which were conducted in the continuous mode of operation. This increase in MSE for the batch experiment may be attributed to an increase in turbulence at the top of the dispersion due to fluctuations caused by slugs exiting the slurry. The MSE for the experiment conducted using a superficial slurry velocity of 0.005 m/s was higher than that for the experiment conducted using a superficial slurry velocity of 0.02 m/s. Increasing the liquid velocity causes a decrease in pressure fluctuations. This decrease in the variance of pressure fluctuations with increasing slurry flow rate may be attributed to two factors: (1) the relative velocity between the gas and slurry decreases with increasing slurry velocity and (2) the static height of the slurry above a given pressure port does not fluctuate as much during a continuous run as it does during a batch run. In Figure 6.7 there is a distinct change in the slope of the curves between gas velocities of 0.02 to 0.04 m/s and 0.06 to 0.12 m/s (i.e. the slopes of curves between gas velocities of 0.06 and 0.12 m/s are greater than the slopes of the curves between gas velocities of 0.02 and 0.04 m/s).. This change in slope may be attributed to a change in the flow regime from bubbly to slug flow. It appears that the transition occurs somewhere between gas velocities of 0.04 and 0.06 m/s for all three experiments. Similar trends were observed in all other experiments conducted. This result agrees with the transition velocities predicted from Taitel et al.'s correlation (i.e., Eq. 6.7).

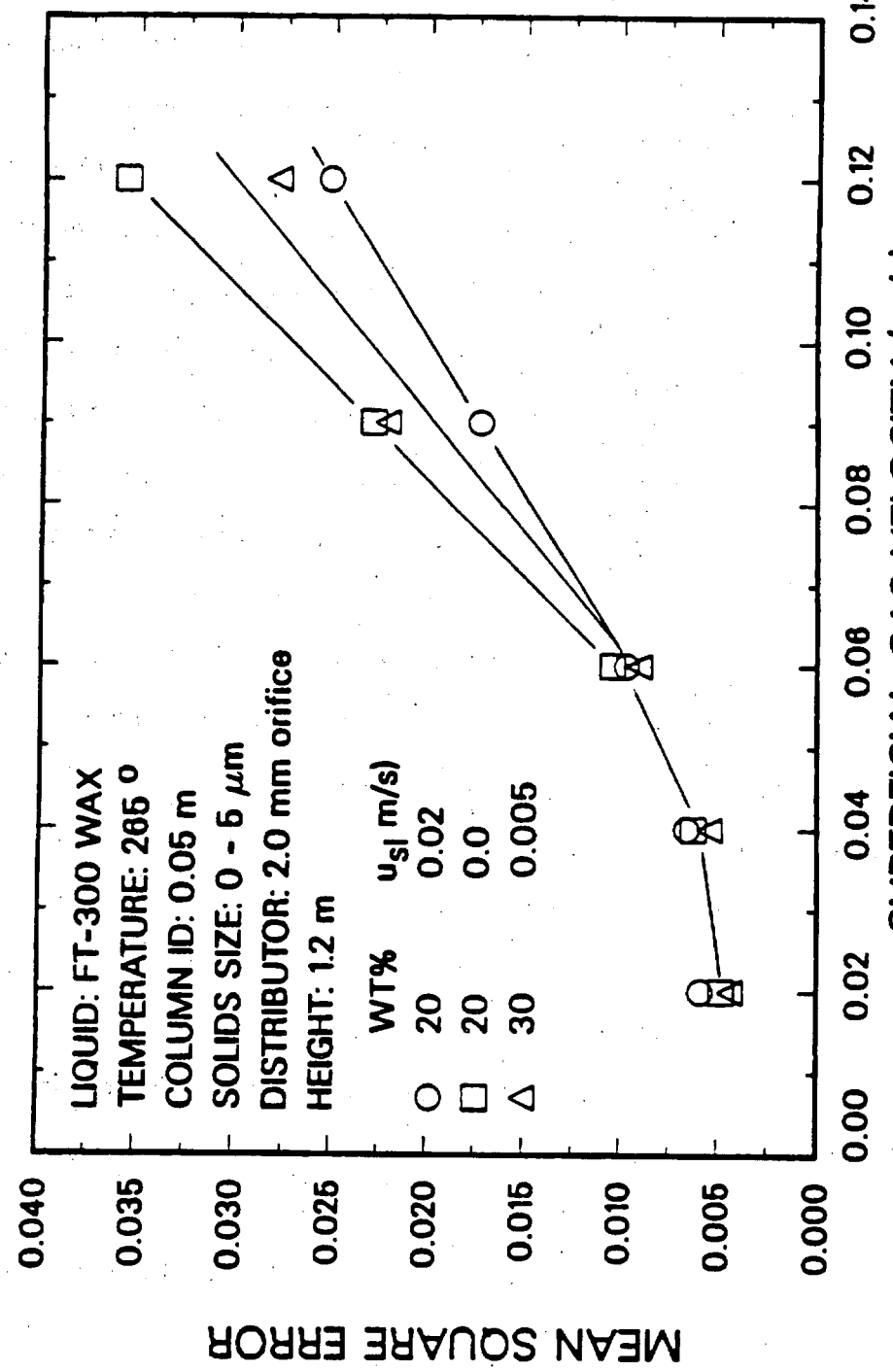

Figure 6.7. Effect of slurry flow rate on the mean square error of pressure fluctuations at the wall (FT-300 wax, 265 °C, 0 - 5 μm silica, 0.05 m ID column, 1.2 m above the distributor).

Figure 6.8 shows the effect of height above the distributor on the MSE at various gas velocities for the batch experiment shown in Figure 6.7. In general, the MSE increases with increasing u_g for all pressure transducers. One interesting trend was the decrease in the MSE between heights of 0.08 and 0.6 m above the distributor. We cannot be certain of the cause for the decrease in MSE at gas velocities of 0.09 and 0.12 m/s. One possible explanation is that the increase in oscillations at a height of 0.08 m is due to the increase in turbulence near the distributor caused by the increase in the gas velocity. The sharp changes in the slope of the MSE curve between heights of 0.6 and 1.2 m at gas velocities of 0.06, 0.09, and 0.12 m/s indicates that slugs begin appearing in the column somewhere between these heights. At gas velocities of 0.02 and 0.04 m/s, there is a slight change in the slope of the MSE curve between heights of 1.2 and 1.8 m, indicating the presence of large bubbles. This result agrees with the prediction of Eq. 6.8, i.e., slugs will not develop in the bottom part of the column.

Figure 6.9 show the effect of superficial gas velocity on the MSE of the pressure fluctuations for the same experiment. At heights of 0.08 and 0.6 m, we do not observe a transition to slug flow; however, the change in slope of the MSE curve for at a height of 1.2 m between gas velocities of 0.04 and 0.06 m/s indicates a transition to slug flow between these velocities. On the other hand, the slope of the MSE curve at a height of 1.8 m above the distributor does not change significantly, indicating that large bubbles are present at all velocities at this height.

Results obtained from experiments with large iron oxide particles showed similar trends in the MSE with gas velocity and height above the distributor. In general, for all experiments in which pressure fluctuations were obtained, the transition between bubbly and slug flow occurred somewhere between gas velocities of 0.04 and 0.06 m/s. Also, slugs were not observed below a height of 0.6 m above the distributor.

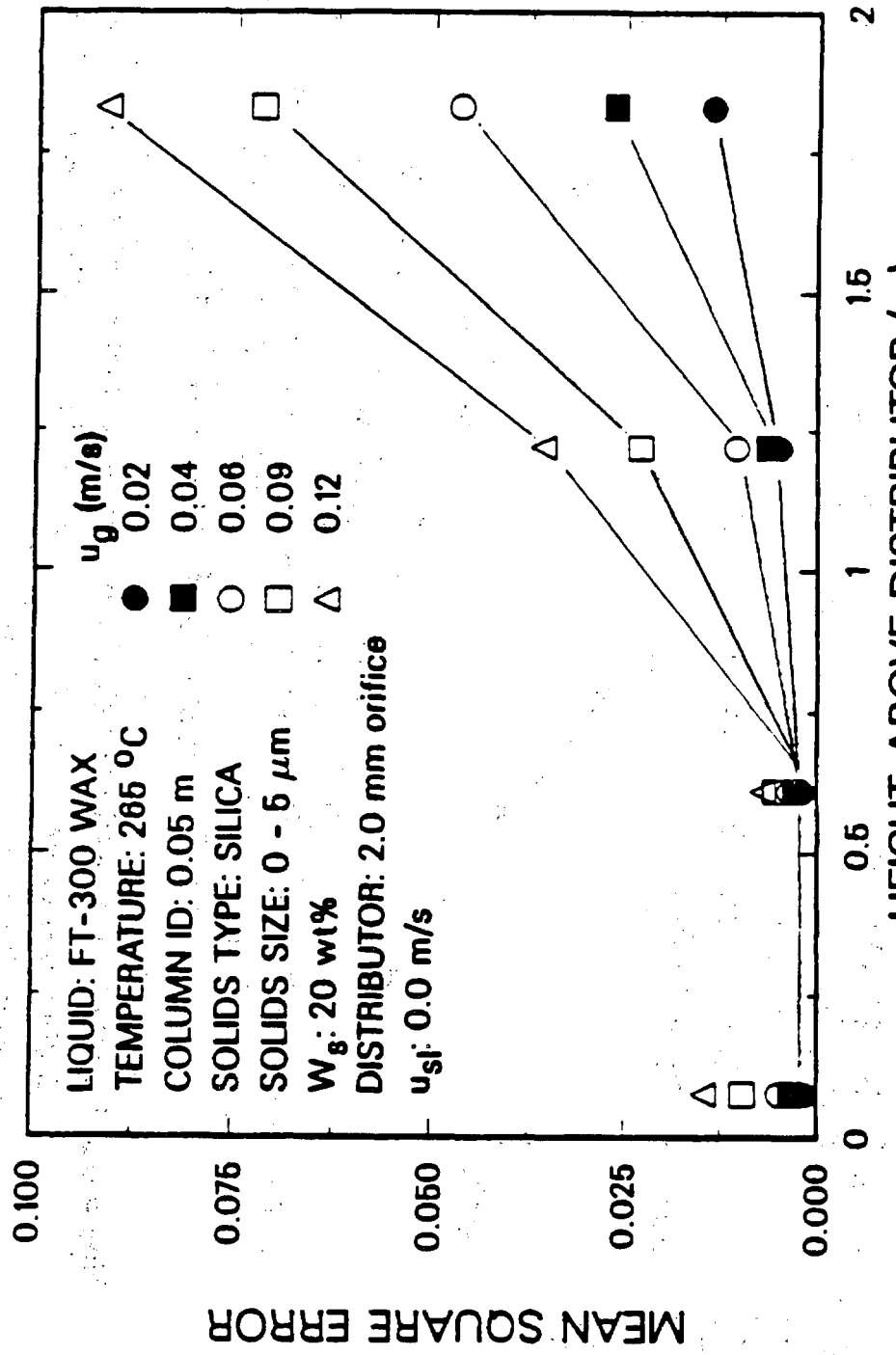

Figure 6.8. Effect of height above the distributor on the mean square error of pressure fluctuations at the wall (FT-300 wax, 265 °C, 20 wt% 0 - 5 μm silica, 0.05 m ID column, u_{sl} = 0.0 m/s).

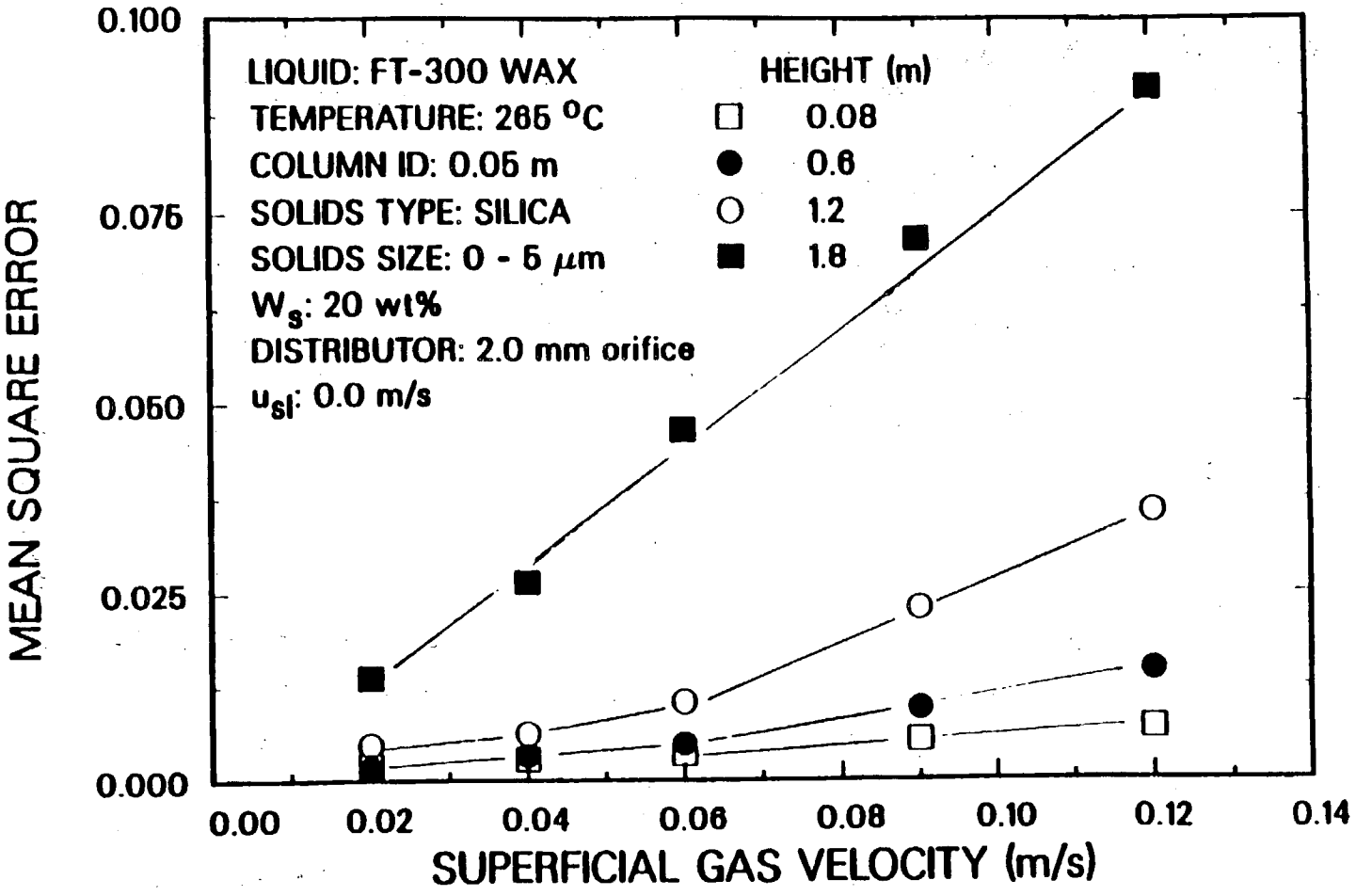

Figure 6.9. Effect of superficial gas velocity on the mean square error of pressure fluctuations at the wall (FT-300 wax, 265 °C, 20 wt% 0 - 5 μm silica, 0.05 m ID column, u_{sl} = 0.0 m/s).

MSE were calculated from both nuclear density gauge signals and raw pressure signals in the 0.21 m ID column for several experiments. In general, the MSE increased with increasing gas velocity but decreased slightly with increasing height above the distributor. Figure 6.10 shows the effect of superficial gas velocity on MSE for nuclear density gauge fluctuations at liquid velocities of 0.005 and 0.02 m/s using the perforated plate distributor and 0.005 m/s using the bubble cap distributor with SASOL reactor wax. An increase in the MSE of nuclear density fluctuations indicates an increase in the variation of gas holdup. For the experiments with the perforated plate distributor there is essentially no effect of liquid flow rate on MSE. However, the MSE of the density gauge fluctuations from the experiment conducted with the bubble cap distributor were significantly lower than those obtained during the experiments with the perforated plate distributor at gas velocities of 0.06 and 0.09 m/s. The lower MSE associated with the bubble cap distributor indicate the presence of a more uniform distribution (i.e. fewer larger bubbles). These results help substantiate the claim that smaller bubbles are formed with the bubble cap distributor due to its geometry. MSE from all experiments were essentially the same at gas velocities of 0.02 and 0.04 m/s. There is a change in the slope of the curves between gas velocities of 0.04 and 0.06 m/s for the experiments conducted with the perforated plate distributor and between gas velocities of 0.06 and 0.09 m/s for the experiment conducted with the bubble cap distributor. The change in slope indicates the transition from the homogeneous bubbly regime to the churn–turbulent flow regime. Similar trends were observed in other experiments. The transition velocities from the bubbly to churn–turbulent flow regime are within the range of velocities given by Deckwer et al. (1980).

Figure 6.11 shows the effect of axial position on the MSE of the pressure fluctuations for the batch experiment conducted with SASOL wax in the 0.21 m ID column. At gas velocities of 0.02 and 0.04 m/s, the MSE of the pressure fluctuations was essentially

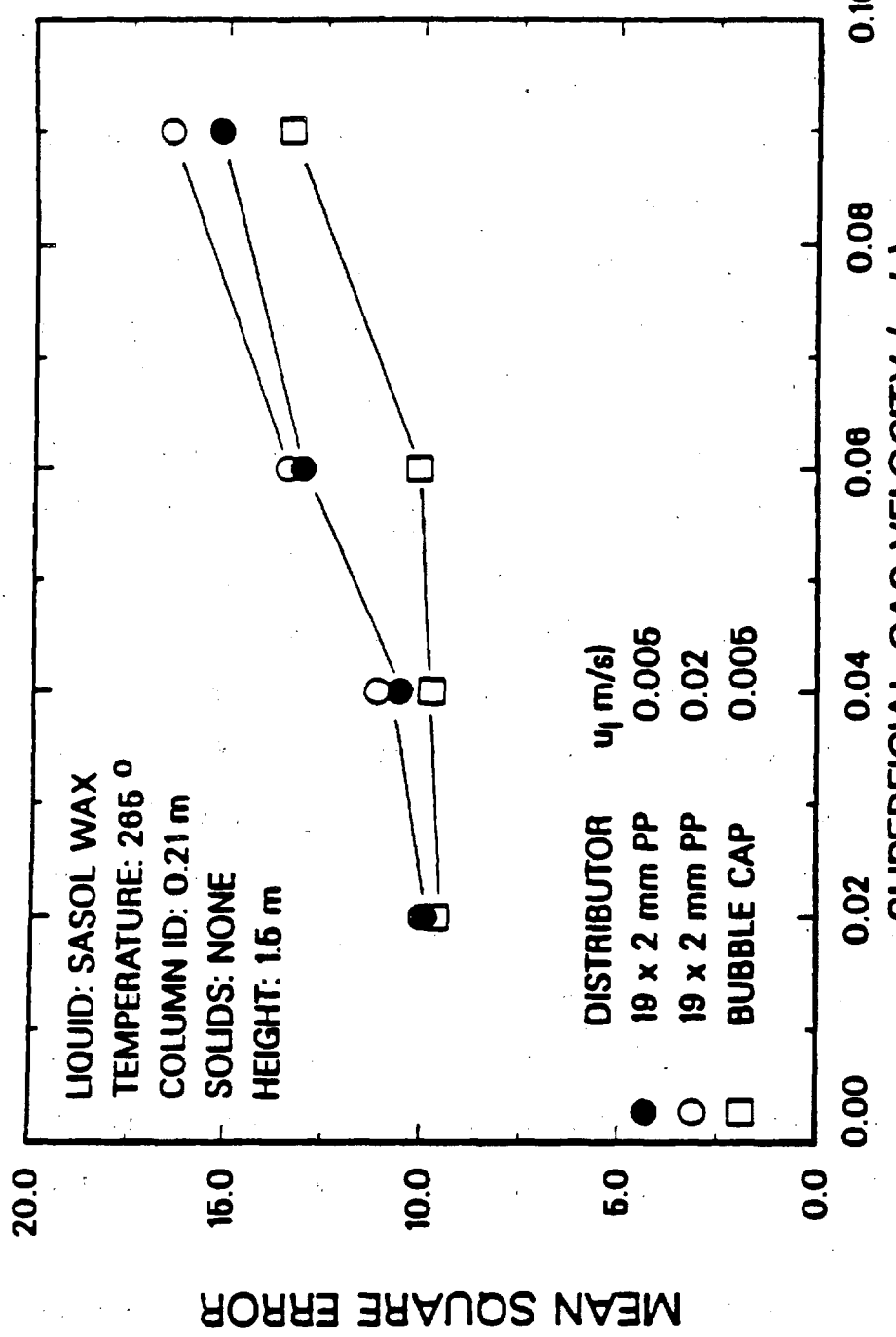

Figure 6.10. Effect of slurry flow rate and distributor on the mean square error of nuclear density gauge fluctuations (SASOL wax, 265 °C, 0.21 m ID column, Cesium-137 source, 1.5 m above the distributor).

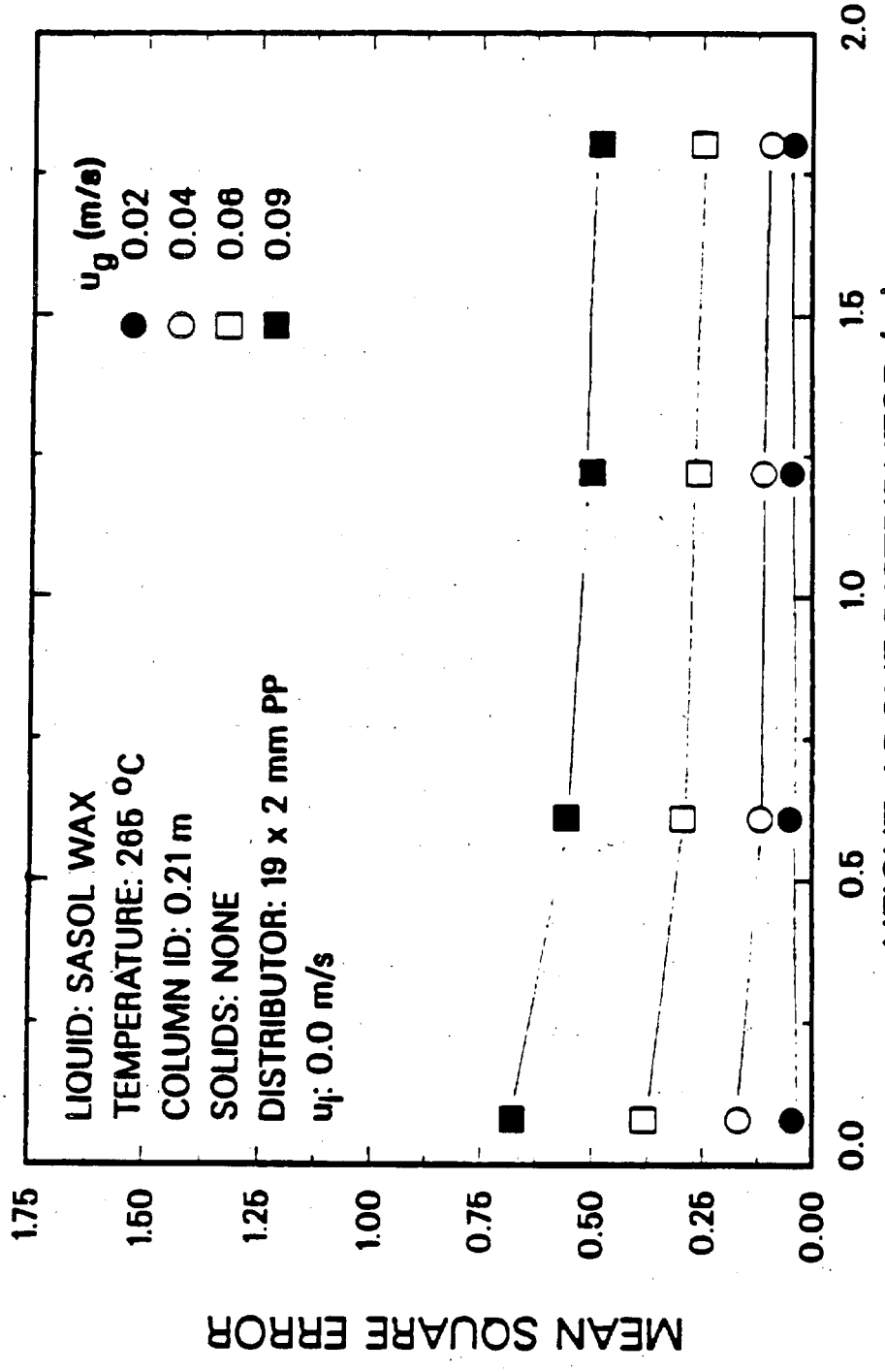

Figure 6.11. Effect of height above the distributor on the mean square error of pressure fluctuations at the wall (SASOL wax, 265 °C, 0.21 m ID column, u_l = 0.0 m/s).

the same at all heights, indicating the presence of the homogeneous bubbly regime. At gas velocities of 0.06 and 0.09 m/s, we observed a slight decrease in the MSE of the pressure fluctuations between heights of 0.08 and 0.6 m above the distributor. A similar trend was observed in the small diameter column (see Figure 6.8). However, in the small diameter column, the MSE increased significantly between heights of 0.6 and 1.2 m above the distributor, but in the large diameter column, it remained essentially constant. The lack of variation in the MSE with column height indicates that there is a minimal amount of axial variation in the flow patterns. We also observed uniform axial gas holdup profiles and bubble size distributions in the large diameter column, which agrees with these results. This type of behavior is representative of the churn–turbulent flow regime.

The effect of superficial gas velocity on the MSE of pressure fluctuations is shown in Figure 6.12 for the batch experiment with SASOL wax in the 0.21 m ID column. As expected, there is an increase in the MSE with increasing gas velocity. The change in slope between gas velocities of 0.04 and 0.06 m/s may be attributed to the transition from the bubbly to the churn–turbulent flow regime. These results are in agreement with those obtained from MSE analysis of nuclear density fluctuations.

Flow Regime Transitions Based on the PSD

Pressure signals and nuclear density gauge signals required high pass filtering. Slow changes in the mean of the signal, unrelated to higher frequency hydrodynamic phenomena, gave rise to a heavy low frequency bias in the psd and autocorrelation functions (Weimer et al., 1985) . To avoid this, the first difference of the time series corresponding to the fluctuations was used before spectra were obtained. The first difference is defined as (Jenkins and Watts, 1968):

$$P'_t = P_{t+\Delta t} - P_t \qquad (6.9)$$

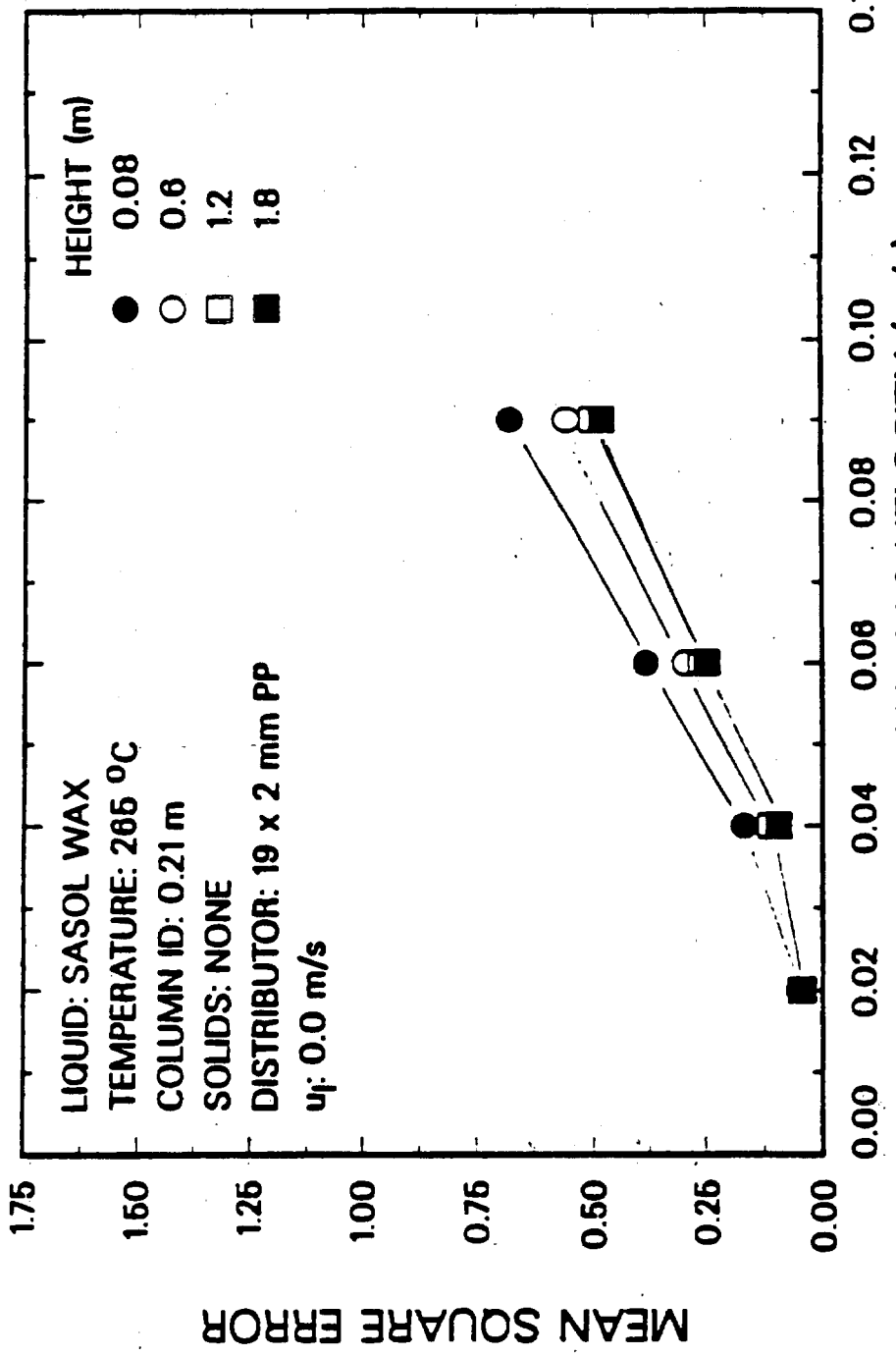

Figure 6.12. Effect of superficial gas velocity on the mean square error of pressure fluctuations at the wall (SASOL wax, 265 °C, 0.21 m ID column, u_l = 0.0 m/s).

where P corresponds to the pressure or nuclear density gauge signal and Δt corresponds to the time difference between two successive measurements. For example, if data was acquired at a rate of 100 Hz, then Δt would correspond to 0.01 sec. The psd was obtained from the new time series, P'_t. The psd of data from experiments with small silica particles and large iron particles in the small diameter column were obtained. The results from these calculations were used to determine flow regime transitions and slug frequencies. Likewise, the psd of data from experiments in the large diameter column in the absence of solids were obtained. These results were used to determine the transition from the bubbly to churn–turbulent flow regime.

Figure 6.13 show spectra of pressure signals obtained at a height of 1.8 m at different gas velocities in the 0.05 m ID column at a superficial slurry velocity of 0.02 m/s. The psd are fairly broad at a gas velocity of 0.02 and 0.04 m/s, with frequencies ranging from 2.5 to 10 Hz. For $u_g \geq 0.06$ m/s, the dominant frequency is in the range 2.5 to 5 Hz. The shift in frequency is indicative of the onset of slug flow between gas velocities of 0.04 and 0.06 m/s. Also, the intensity of the psd increases with increasing gas velocity; a similar trend was observed with the MSE (i.e. MSE increased with increasing gas velocity).

The spectra from transducers at heights of 0.6, 1.2, and 1.8 m above the distributor at a gas velocity of 0.12 m/s for the batch experiment conducted with 20 wt% 20 – 44 μm iron oxide particles in the 0.05 m ID column are shown in Figure 6.14. The dominant frequency observed at a height of 0.6 m above the distributor is 5 Hz; whereas, the dominant frequency at heights of 1.2 and 1.8 m is 2.5 Hz. This shift from 5 Hz to at the bottom of the column to 2.5 Hz at the top of the column is an indication of coalescence which may be taking place. Similar results were observed for the batch experiment with small silica (see Figure 6.15). For experiments conducted in the glass column we observed slug frequencies in the range 2 to 3 Hz at the top of the column

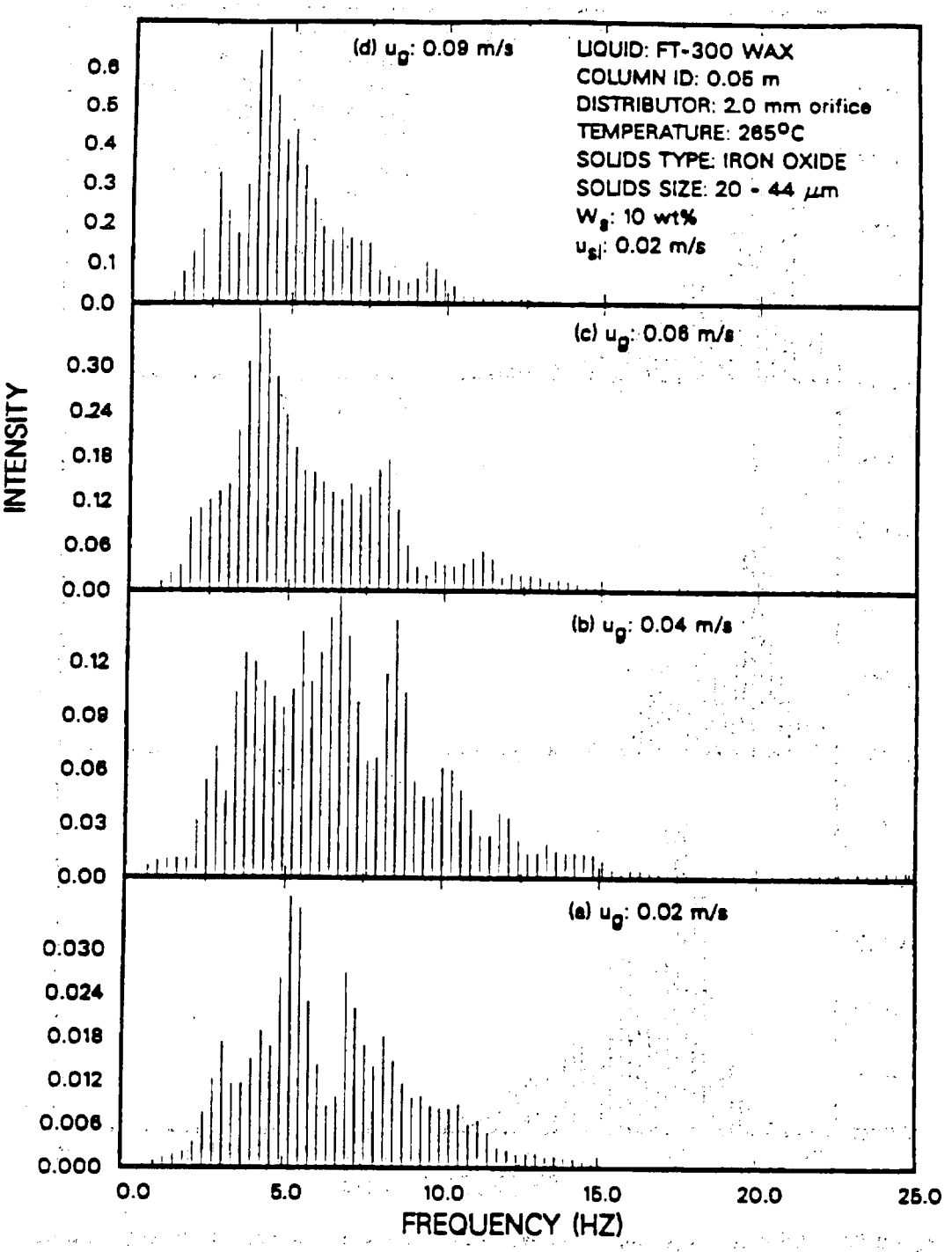

Figure 6.13. Effect of superficial gas velocity on the power spectral density function for pressure fluctuations at the wall (FT-300 wax, 265 °C, 0.05 m ID column, 10 wt% 20 - 44 μm iron oxide, u_{sl} = 0.02 m/s, height = 1.8 m).

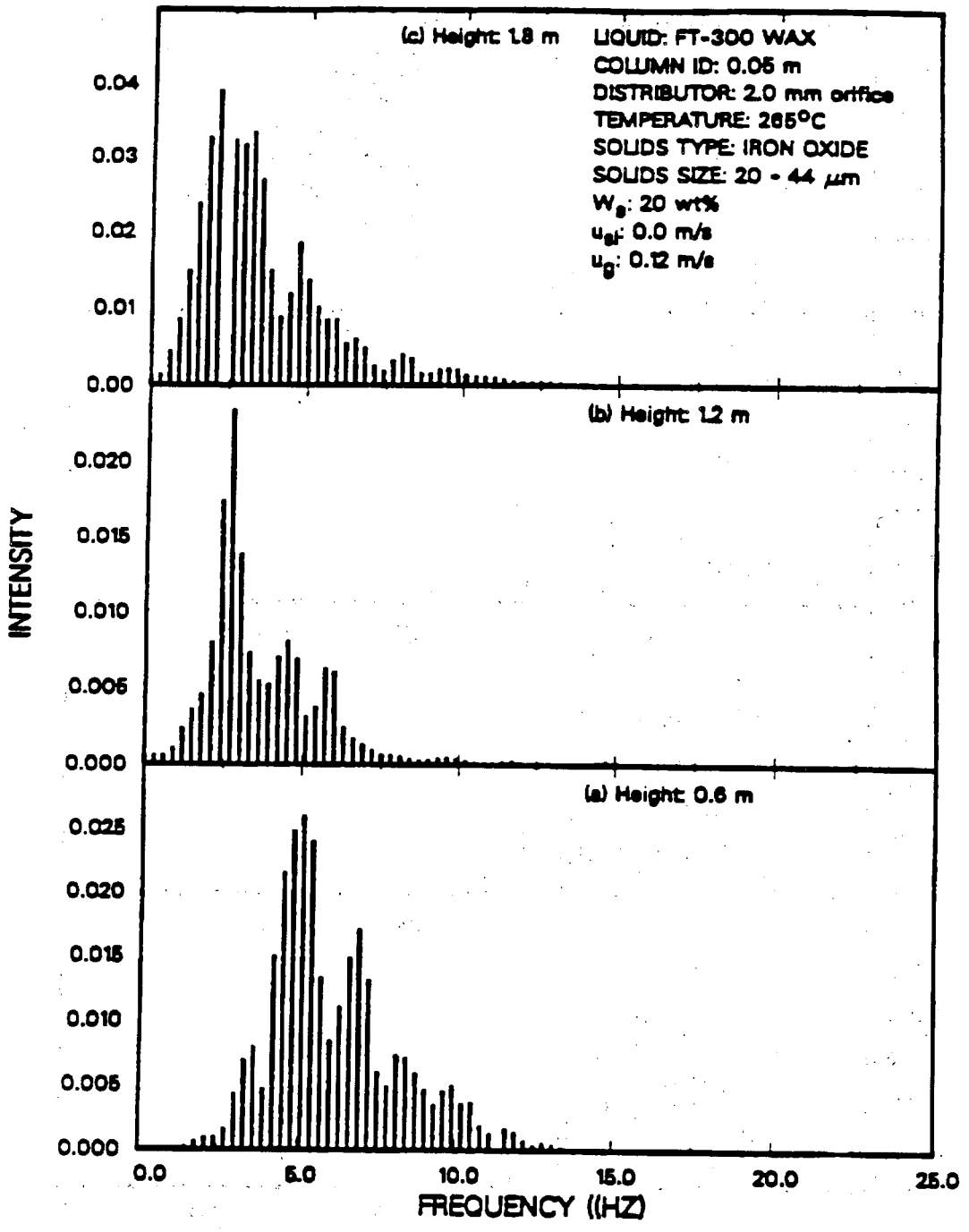

Figure 6.14. Effect of height above the distributor on the power spectral density function for pressure fluctuations at the wall (FT-300 wax, 265 °C, 0.05 m ID column, 20 wt% 20 - 44 μm iron oxide, u_{sl} = 0.0 m/s, u_g = 0.12 m/s).

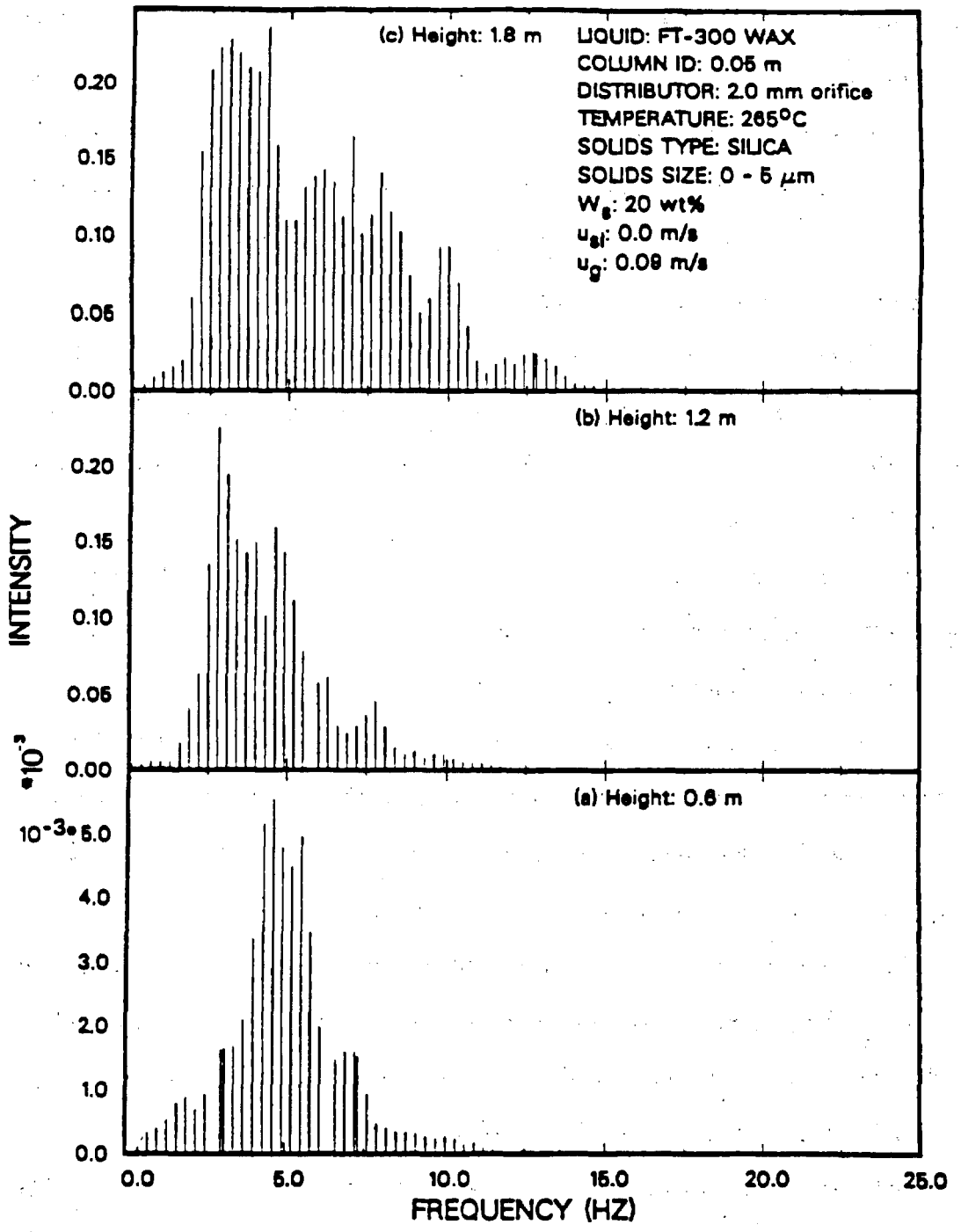

Figure 6.15. Effect of height above the distributor on the power spectral density function for pressure fluctuations at the wall (FT-300 wax, 265 °C, 0.05 m ID column, 20 wt% 0 - 5 μm silica, u_{sl} = 0.0 m/s, u_g = 0.09 m/s)

for gas velocities of 0.07, 0.09, and 0.12 m/s. At the bottom of the column, we have more frequent, smaller slugs, whereas, towards the top of the column, two small slugs coalesce to form a single large slug. This type of behavior has been observed visually in our two–phase experiments conducted in the glass column. This also agrees with the description proposed by Taitel et al. (1981) which was used in their correlation for determining the entry region over which churn flow exists.

Thus, for experiments conducted in the small stainless steel column in the batch mode of operation, the dominant slug frequency is approximately 2.5 Hz at the top of the column. Coalescence of small slugs to form large slugs occurs between a height of 0.6 m and 1.2 m above the distributor.

Figure 6.16 shows the effect of superficial gas velocity on the psd of the nuclear density gauge fluctuations from the batch experiment with FT–300 wax (without solids) in the small diameter column at gas velocities of 0.02, 0.04, 0.06, and 0.09 m/s. The four plots at the four different gas velocities indicate the progressive movement of the dominant frequency to the left (towards lower values) with an increase in gas velocity. These results show that the spectra are narrower at higher gas velocities (u_g=0.06 and 0.09 m/s) than they are at lower velocities. This behavior in the frequency spectrum is indicative of the change in flow regime in the bubble column. At low gas velocities, the homogeneous bubbly regime prevails and goes through a transition before approaching the slug flow regime at a gas velocity of 0.06 m/s. The dominant frequency at a gas velocity of 0.02 m/s is in the range 7.5 to 10 Hz, and shifts to the range 2.5 to 5 Hz at 0.04 m/s, and finally approaches 2.5 Hz as slug flow develops at 0.06 m/s. The definite shift in the dominant frequency observed between gas velocities of 0.04 and 0.06 m/s which was observed in all experiments indicates that slug flow begins somewhere between these two velocities. As mentioned previously, the same transition region was observed in experiments with the silica particles using MSE analysis (see Figure 6.9).

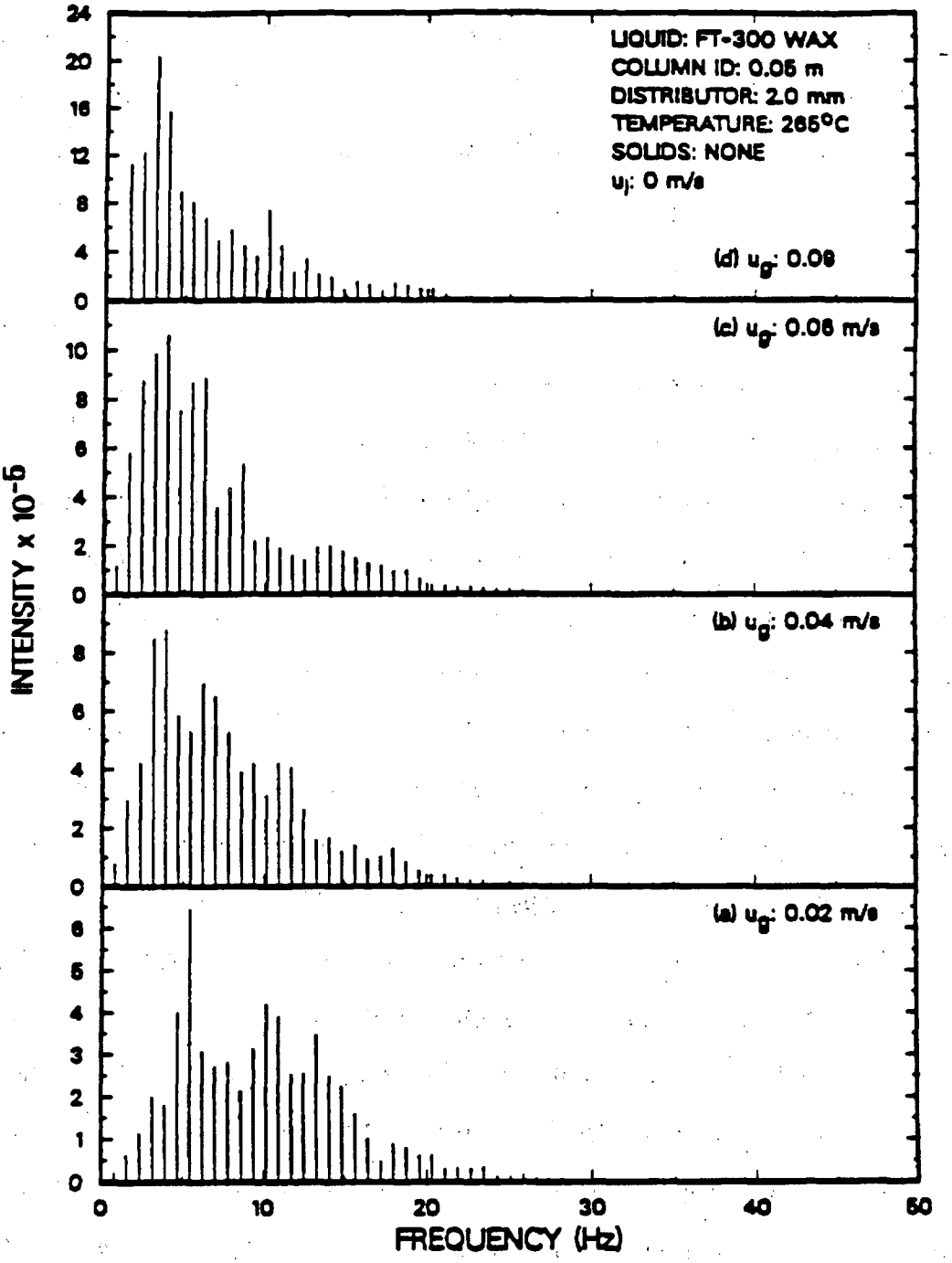

Figure 6.16. Effect of superficial gas velocity on the power spectral density function from the nuicear density gauge (FT-300 wax, 265 °C, 0.05 m ID column u_l = 0.0 m/s, Cesium-137, height = 1.5 m).

Hence, both MSE and psd analysis may be used to determine the transition from bubbly to slug flow. In addition, the psd may be used to determine slug frequency. Results obtained from statistical analysis results are in agreement with predictions from Taitel et al.'s correlations. Also, they are consistent with our visual observations in the small glass column.

The effect of superficial gas velocity on the power spectra for pressure signals obtained from the batch experiment with SASOL reactor wax (no solids) in the 0.21 m ID column at heights of 0.08 and 1.8 m above the distributor are shown in Figures 6.17 and 6.18, respectively. In the vicinity of the distributor, two characteristic psd peaks are observed (see Figure 6.17). The bimodal distribution may be indicative of the coalescence near the distributor. The intensity of the low frequency peak increases significantly with increasing gas velocity, which implies the formation of larger, less frequent bubbles in the vicinity of the distributor. At a height of 1.8 m above the distributor, a single peak in the psd is observed. The single peak is representative of a stable flow pattern (i.e. stable bubble size). As the gas flow rate is increased from 0.02 to 0.04 m/s, there is a definite shift in the frequency of the psd (12 Hz at 0.02 m/s to 8 - 10 Hz at 0.04 and 0.06 m/s). This shift in the dominant frequency between gas velocities of 0.02 and 0.04 m/s represents the transition from bubbly to the churn–turbulent flow regime.

Figures 6.19 and 6.20 show the effect of height above the distributor on the psd for the same experiment at gas velocities of 0.02 and 0.06 m/s, respectively. At both velocities, the bimodal distribution prevails at heights of 0.08 and 0.6 m. As mentioned above, the bimodal distribution is characteristic of the entry region over which bubble coalescence and breakup occurs. At heights of 1.2 and 1.8 m above the distributor, we no longer observe the bimodal distribution, thus indicating the presence of fully developed flow.

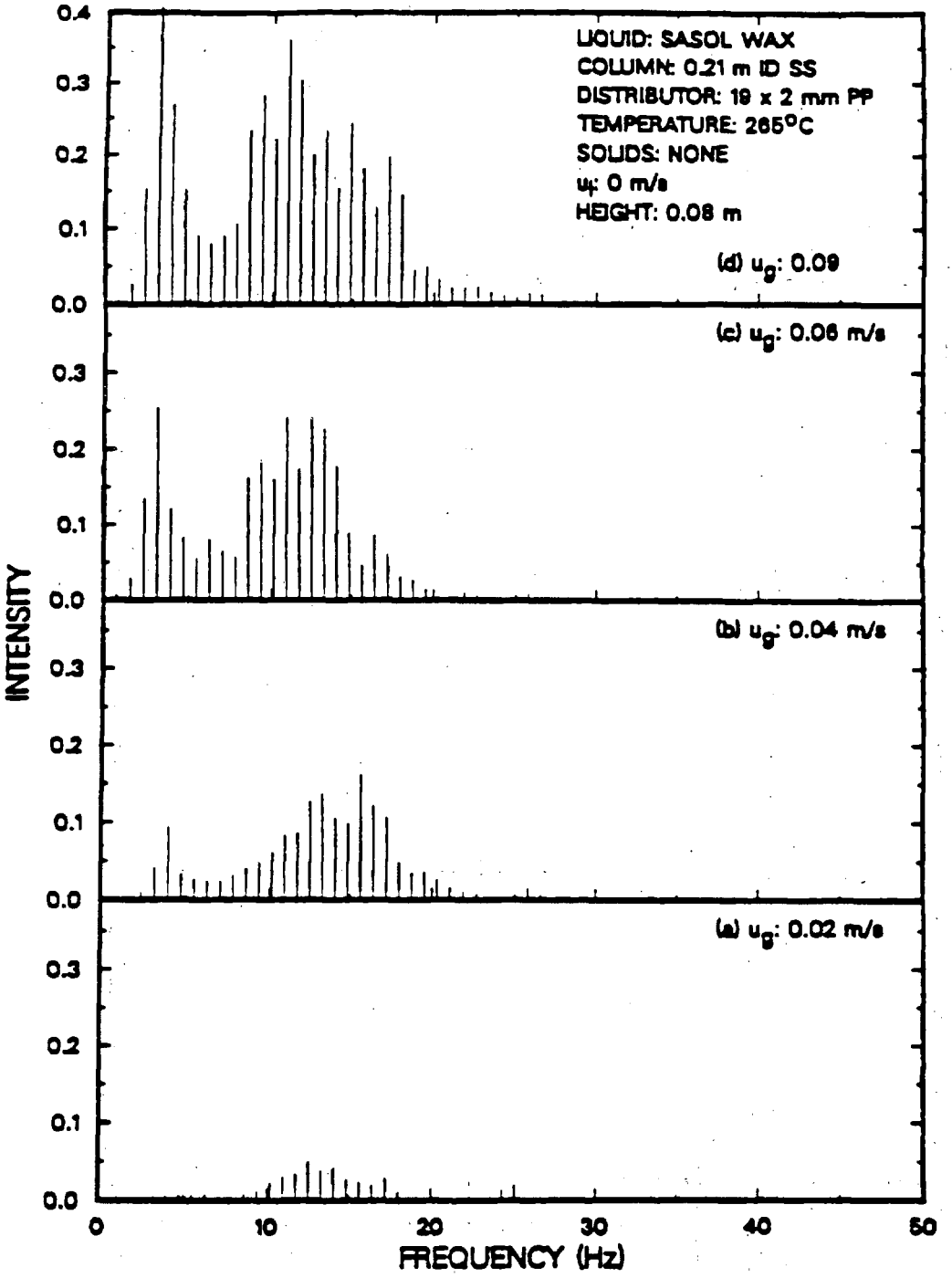

Figure 6.17. Effect of superficial gas velocity on the power spectral density function for pressure fluctuations at the wall (SASOL wax, 265 °C, 0.21 m ID column, u_l = 0.0 m/s, height = 0.08 m).

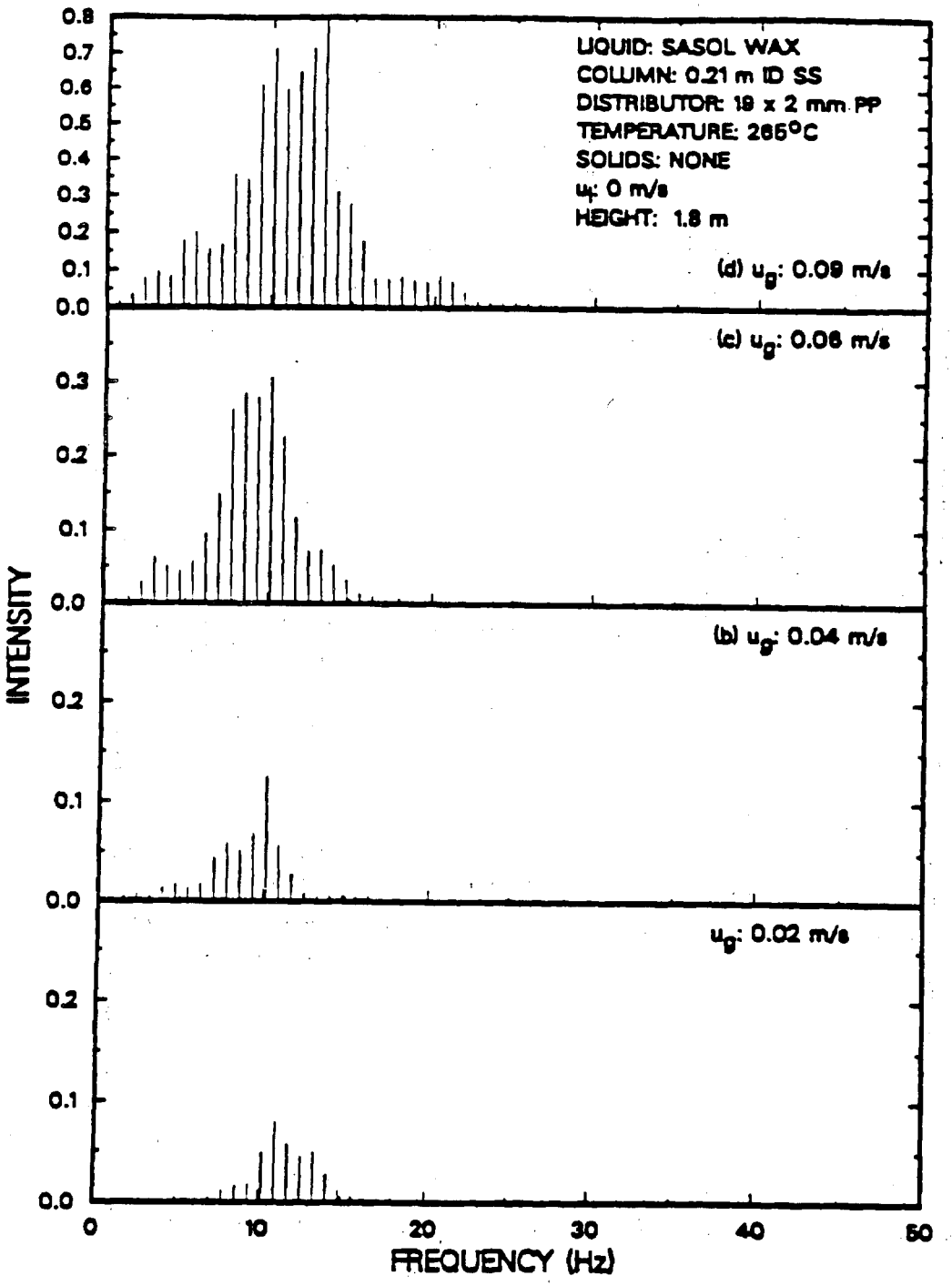

Figure 6.18. Effect of superficial gas velocity on the power spectral density function for pressure fluctuations at the wall (SASOL wax, 265 °C, 0.21 m ID column, u_l = 0.0 m/s, height = 1.8 m).

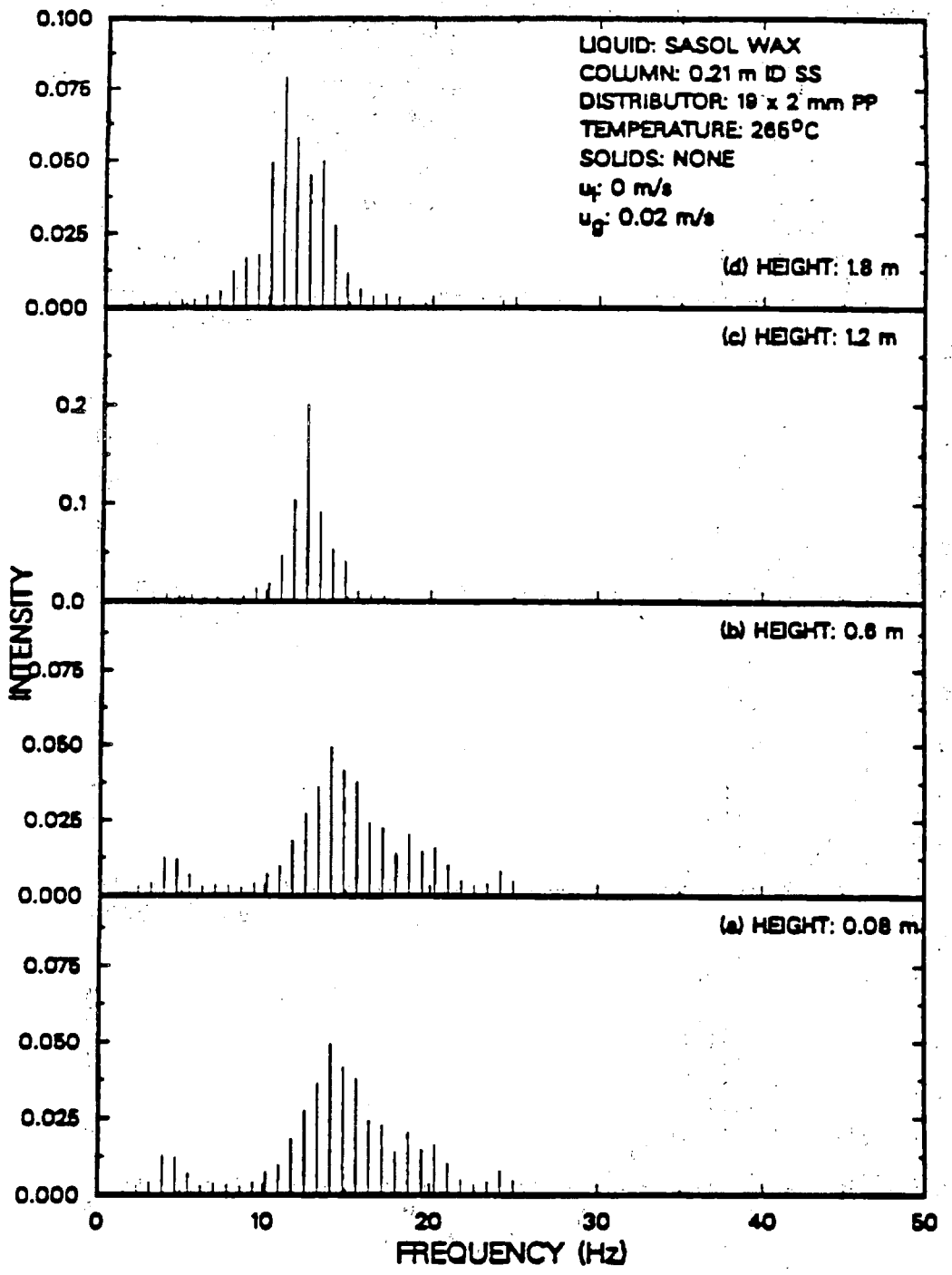

Figure 6.19. Effect of height above the distributor on the power spectral density function for pressure fluctuations at the wall (SASOL wax, 265 °C, 0.21 m ID column, u_l = 0.0 m/s, u_g = 0.02 m/s).

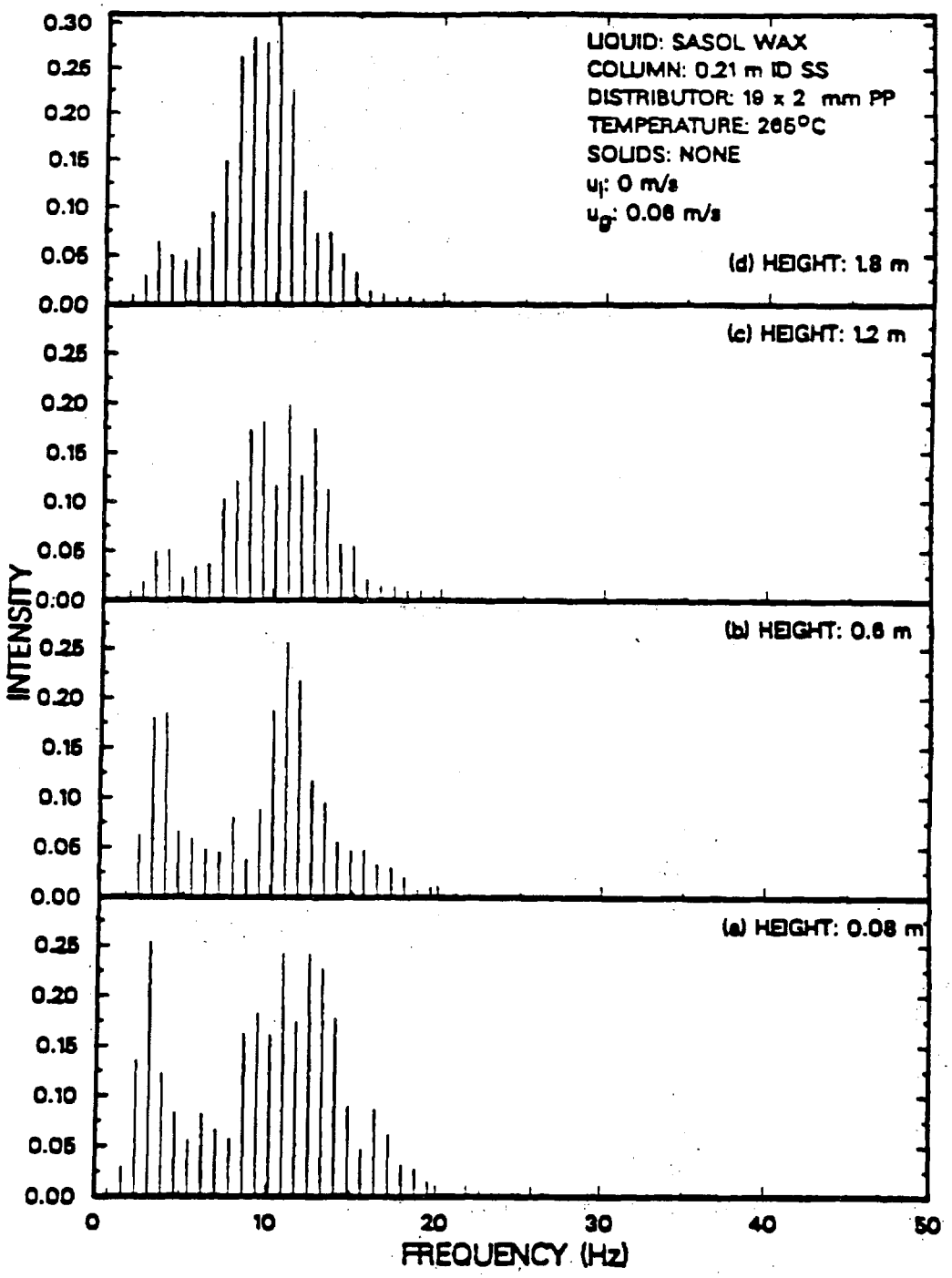

Figure 6.20. Effect of height above the distributor on the power spectral density function for pressure fluctuations at the wall (SASOL wax, 265 °C, 0.21 m ID column, u_l = 0.0 m/s, u_g = 0.06 m/s).

Figure 6.21 shows the effect of superficial gas velocity on the psd of nuclear density gauge fluctuations from the batch experiment with FT–300 wax in the 0.21 m ID column at a height of 1.5 m above the distributor. At a gas velocity of 0.02 m/s, the psd is fairly broad, which indicates the presence of the homogeneous bubbly regime. As the gas velocity is increased, the psd appears to become narrower and there is a shift in the dominant frequency towards the left (i.e. lower frequency). In the homogeneous bubbly regime, there is not a dominant frequency; however, in the churn–turbulent flow regime, large bubbles are produced which pass by the transducer at regular intervals (i.e. the dominant frequency). At a gas velocity of 0.02 m/s the frequency primarily ranges from 6 to 12 Hz; whereas, at gas velocities of 0.04 and 0.08 m/s, the dominant frequency is approximately 6 Hz. This shift in the frequency of the psd represents a transition from the bubbly flow regime to the churn–turbulent flow regime. The transition to the churn–turbulent flow regime in the neighborhood of 0.04 m/s is in agreement with our results obtained using the MSE approach. Also, the transition velocity is within the range of velocities presented by Deckwer et al. (1980).

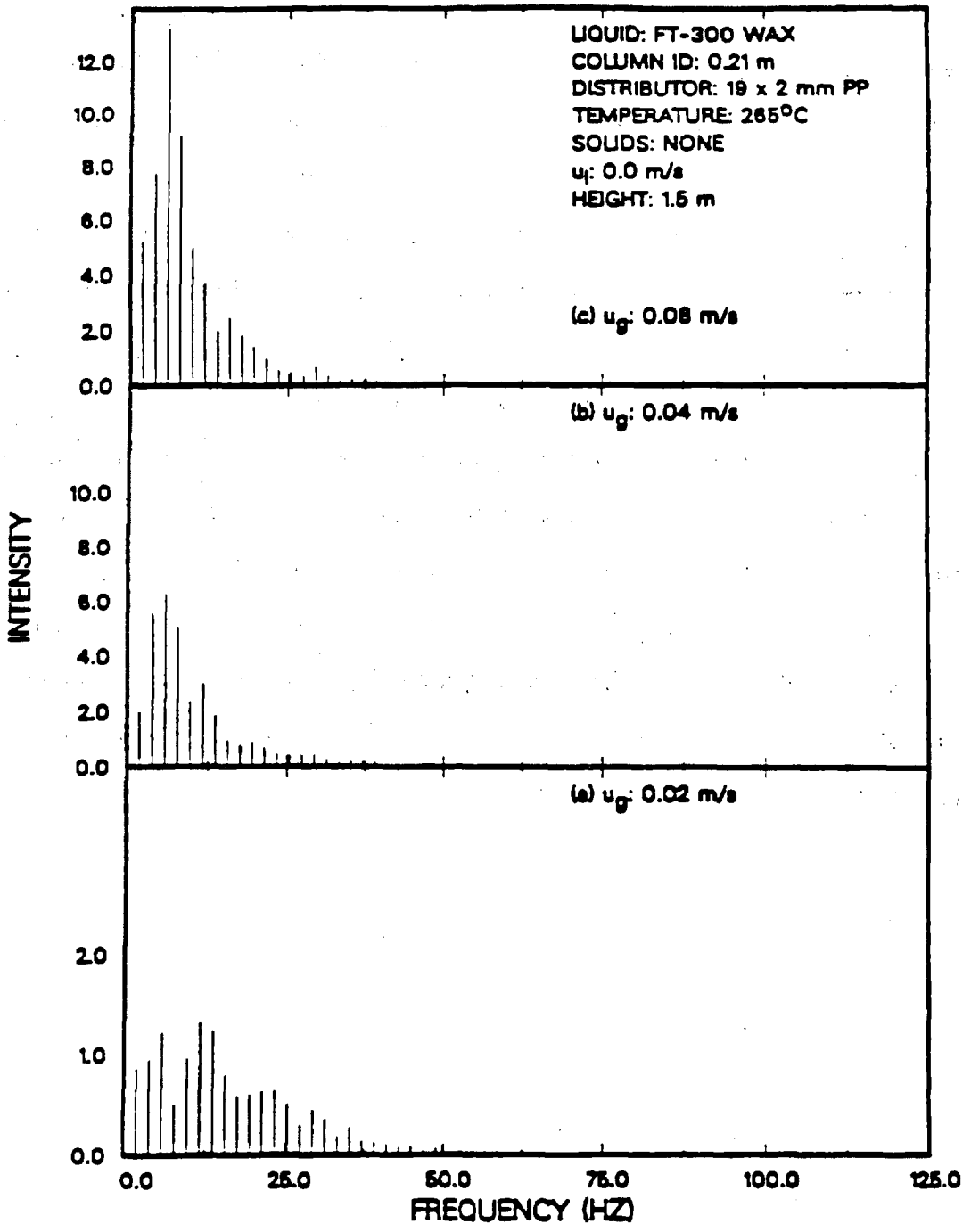

Figure 6.21. Effect of height above the distributor on the power spectral density function for nuclear density gauge fluctuations (FT-300 wax, 265 °C, 0.21 m ID column, Cobalt-60, height=1.5 m).